GEOLOGY OF THE ELISENHEIM AREA, WINDHOEK DISTRICT, SOUTH WEST AFRICA, WITH SPECIAL REFERENCE TO THE MATCHLESS AMPHIBOLITE BELT

by

S.H. FINNEMORE B.Sc. (HONS)

Thesis submitted for the degree of
Master of Science at Rhodes
University, Grahamstown

June 1974.

ABSTRACT

The Elisenheim area is situated just north of Windhoek within the Windhoek Formation of the Swakop Subgroup and is underlain by monotonous succession of semi-pelitic schists with intercalations of amphibolite, talc schist, graphitic schist and marble. Petrographic studies on units of the Matchless amphibolite which outcrop in the south of the property, have resulted in the recognition of three different types of amphibolite, namely, epidote amphibolite, porphyroblastic amphibolite and chlorite-amphibole schist. Amphibole porphyroblasts generally display patchy and zonal intergrowths of hornblende and actinolite which are indicative of non-equilibration during prograde metamorphism. Talc schists have been mapped in the north of the property.

All lithotypes have undergone three phases of deformation (F_1, F_2, F_3) which terminated with the faulting which underlies the Klein Windhoek, Dŏbra, Tigenschlücht and Kuruma rivers.

Medium grade regional metamorphism accompanied F_1, F_2 and F_3 and outlasted the latter. Mineral assemblages throughout the area are those of the amphibolite facies and P,T conditions prevailing during metamorphism are estimated to have been at least 5 kb at $\sim 550^{\circ}C$.

Petrochemical evidence indicates that the Matchless amphibolites are igneous in origin and genetically related to the ultrabasic talc schists. They are similar in composition to oceanic tholeiites and are thought to have been extruded subaqueously.

CONTENTS

INTRODUCTION

1.1. General

The area investigated during this survey (Map 1) is situated just north of Windhoek and covers the farm Elisenheim 68 which lies on the eastern side of the Windhoek-Okahandja national road within the Eros Mountains.

1.2. Previous Work

Portions of the Windhoek district have been previously described by various writers, none of whom studied the Elisenheim area in detail. The first comprehensive study of the Windhoek district was carried out by Gevers (1934). Guj (1967) described the structural geology of the Auas Mountains which lie south of Windhoek and Hälbich (1970) presented a structural-stratigraphic analysis of the western Windhoek-Rehoboth districts.

1.3. Present Investigation

The material used in this study was gathered during a period of six months spent by the writer prospecting on the property for Newmont South Africa Limited. During this time, mapping of the property with the aid of aerial photographs, on a scale of 1 : 25 000, was completed. Detailed mapping on a scale of 1 : 1 000 in the vicinity of the Matchless Amphibolites and the dolomitic talc schists plus reconnaissance of neighbouring properties on a scale of 1 : 25 000 was also undertaken.

Laboratory work and structural, petrographic, metamorphic and petrochemical interpretations were made at Rhodes University. It is hoped that these findings, especially the petrochemical data, will prove useful in other studies.

1.4. Acknowledgements

The writer wishes to express his gratitude to a number of persons and organisations for assistance given during the course of this project. Firstly, to Dr. R.E. Jacob of the Department of Geology, Rhodes University, under whose supervision the investigation was made and for many valuable discussions and for editing the various drafts. Special thanks are due to Dr. J.S. Marsh of the Department of Geology, Rhodes University, Mr. V. Vellet of Newmont South Africa Limited and Dr. A.L. Paverd, formerly of Newmont, for many discussions in the laboratory and field. The National Institute for Metallurgy is thanked for the chemical analyses.

It is a pleasure to acknowledge the financial support of Newmont South Africa Limited for the project. Thanks are due to Mr. R. Teichmann and Mr. G. Dodds of Matchless Mine for providing many rock samples and access to unpublished material. Thanks, too, are due to Mrs. A. Wicks for typing the manuscript.

2. FIELD RELATIONSHIPS AND STRATIGRAPHY

2.1. Classification and Nomenclature

The stratigraphy of the Damara orogen has been subdivided by Hälbich (1970) on a chronostratigraphic basis. His subdivision, in the Windhoek area, of what he termed the Damara System is shown in Table 1. This terminology has been superceded by the proposals of the S.A.C.S. Working Group post-Waterberg/pre-Cape (Kröner et al., 1974). The two classifications do not differ much except in the adoption of the nomenclature group/subgroup/formation for facies/series/stage and the substitution of Chuos Formation for Onnaams Stage as the lowest member of the Khomas Subgroup.

The term "Matchless Amphibolite" is applied to the conspicuous zone of amphibolitic rocks up to 2 km wide, that strike ENE for a distance of 300 km from the Kuiseb River in the southwest to the Steinhausen area in the northeast, and which was previously named the "Friedenau Amphibolite" by Hälbich (1970). The rocks of the Elisenheim area lie within the lower portion of the Windhoek Formation.

2.2. Khomas Subgroup

The Khomas Subgroup is made up of the Chuos, Auas and Windhoek Formations (Kröner et al, 1974) and is comprised largely of a monotonous sequence of quartz-feldspar-biotite schists derived essentially from greywackes, sub-greywackes and shales.

The Chuos and Auas formations crop out south of Windhoek and the quartzitic Auas formation forms the Auas Mountains. The base of the Windhoek formation outcrops just south of Windhoek and marks the beginning of a monotonous sequence of mica schists which outcrop continuously over large areas and underlie the entire Khomas Highlands to the west of Windhoek and the Eros mountains to the north and east. The Matchless amphibolite belt constitutes a distinctive and well-demarcated stratigraphic component (see Figure 18) and is made up largely of bands and lenses of amphibolite, amphibolitic schist and talc schist and is often accompanied along strike by lenses of sericitic quartzite. A number of graphitic schist horizons are developed mainly towards the north (Viljoen et al, 1975) and along with the amphibolite belt are the only recognizable stratigraphic units within the Windhoek formation. The Windhoek formation disappears further to the north near the centre of the Damara orogen (in the vicinity of Okahandja) and is replaced by a zone of granites and higher grade metamorphic rocks. Granitic rocks representing both basement and anatectic varieties as also present south of the Auas mountains. The Khomas subgroup is considered to form part of an elongated trough of sediments and volcanics of probable eugeosynclinal type confined by regional tectonic basement highs lying to the north and south (Viljoen et al, 1975).

Examination of ERTS imagery shows that the Khomas subgroup is characterised by a strong linearity in an ENE-WSW direction with very little indication of open folding. This pattern, according to Viljoen et al (1975), is in marked contrast to the tectonic style of the central portion of the Damara orogen, that lies to the north of the Khomas Subgroup, and

that is characterised by numerous eye-type folds (in an area of higher grade metamorphism and intrusive anatectic granites).

2.2.1. Windhoek Formation

This formation underlies the Elisenheim area and consists largely of a monotonous succession of various mica schists and soft sericitic quartzites containing occassional bands of amphibolite, graphitic schist and carbonated talc schist. The most prominent of the amphibolites is the Matchless belt which outcrops in the extreme south of the property.

Quartz-biotite schists and micaceous "quartz-augen" schists are isoclinaly folded and display a prominent northwards dipping (transposition) foliation. It is not possible to separate the two units on a regional scale as they form an indistinguishable mass (see Plate 3) of transposed schists. Contacts between the two schists are transposed. The difference in texture, mineralogy and style of folding between the quartz biotite schists and micaceous "quartz-augen" schists appears to be a tectonic feature caused by the incompetency of the latter horizon relative to the former.

The Matchless belt generally consists of two or three bands

	Hälbich (1970)			Kröner et al (1974)		
DAMARA SYSTEM	Series	Stage		SWAKOP GROUP	Subgroup	Formation
	KHOMAS	Windhoek			KHOMAS	Windhoek
		Auas				Auas
		Onnaams				Chuos
	DISCORDANCE					
	HAKOS	Berghof			HAKOS	Berghof
		Verloren				Verloren

Table 1. Stratigraphic terminology for the Damara rocks of the Damara Orogen in the Windhoek area.

(with outcrop widths ranging between 2 m and 100 m) spread over a zone 1500 m wide. The amphibolites have been traced from the Khomasdal and Katatura townships to north of Otjihase Mine and have been faulted in step-like fashion by faults underlying the Klein Windhoek, Döbra, Tigenschlücht and Kuruma rivers. The amphibolites lie conformably within the schists and have undergone transposition which accounts for the "braided" pattern of outcrop shown on map 1. The belt is comprised largely of coarse-grained porphyroblastic amphibolite which has a spotted appearance in outcrop. Epidote amphibolite, which often displays boudinage structures, and chlorite-amphibole schist are intercalated within the northern and central units of the belt east of the Döbra River. Highly crenulated chlorite-amphibole schist was also mapped within these units near the Daan Viljoen Game Reserve, 15 km to the west of Elisenheim. Changes in lithology within various amphibolite bands are generally obscured by the rubble and scree prevalent on the mountain slopes but are most noticeable in the two northern bands. Textural changes in the porphyroblastic amphibolites are restricted to shearing on the margins of the bodies which are generally massive and only slightly foliated.

Talc schists are present in the northwestern corner of Elisenheim, 7 km north of the Matchless amphibolite belt. The talcose rocks outcrop in a body measuring 150 m x 300 m which is elongated in a northwesterly direction discordantly across the regional strike. The body is highly folded and contorted and contains abundant small-scale B_2 folds. Contacts between the talc schists and surrounding quartz biotite schists are generally covered by alluvium. The talcose body consists of intricately-mixed bands of talc schist, dolomitic talc schist, talc-chlorite schist, chlorite-actinolite schist, quartz-chlorite-magnetite schist and rare lenses of brown marble. A characteristic feature of the body is the abundance of dolomite porphyroblasts which have grown across the S_3-foliation in the talc schists whichare also sparsely mineralised by flakes of malachite and specks of oxidized sulphides. Massive quartz veins rich in chlorite are scattered throughout the ultramafics. Talc schists are also found in the vicinity of the amphibolites at Otjihase Mine.

All samples of schist and amphibolite obtained from Matchless Mine are identical texturally and mineralogically to those from Elisenheim.

A narrow band of graphitic schist (2 m) crops out conformably within the semi-pelitic mica schists east of Elisenheim. This lithotype is mappable for 2,5 km from the Elisenheim boundary to the Tigenschlücht River where it is truncated by a north-trending fault which is downthrown in the west. No trace of the horizon was found east of the fault where a band of magnetite outcrops in association with a lens of actinolite schist. The quartzite is contorted and folded and contains partings of iron oxide. Small intercalations of marble, not mappable on the scale of Map 1 were found scattered within the Elisenheim schists.

The area mapped is cut by four major north-trending faults which are marked by river beds and gorges. Prominent horizons of mylonite mark the fault zones.

3. STRUCTURE

3.1. Introduction

Three phases of tectonic deformation have been recognised in the Elisenheim area despite the fact that most structures have been appressed and sheared out, producing perfect examples of transposition foliation. All the schists consequently exhibit a prominent northwards-dipping foliation and strike ENE-WSW. Regional mapping was carried out on a scale of 1 : 25 000 by conventional mapping techniques and was followed by structural analysis of the fabric elements of the rocks. The transposed nature of the beds and the absence of definite markers within these Khomas schists have prevented the mapping of large scale structures. The aim of field work under such conditions, therefore, was mainly to obtain, on the basis of structural analysis, a three-dimensional picture of all the visible structural elements and to determine the deformation sequence in the rocks.

Portions of the Windhoek district have been previously described by various writers including Gevers (1934), Guj (1967) and Hälbich (1970).

Gevers (1934) only briefly described the tectonic features of the area while Guj (1967) discussed the structures of the Auas Mountains south of Windhoek. Guj (1967) claims that after initial folding and recrystallisation of the Auas sediments, continued stress led to a southerly directed thrust of the plastically folded sediments over the more competent granitic rocks of the southern area. The resistance of the infrastructure to the movement of the overriding thrust sheet laterally gave rise to different types of folds which can be classified into four different structural zones. The transition between any two of these adjoining zones is not gradual according to Guj (1967) but is marked by a north-striking tear- or transcurrent-fault. The northern extensions of these faults are the only structures dealt with by Guj (1967) that are present within the Elisenheim area.

The structural analysis undertaken by Hälbich (1970) in the southern marginal zone of the Damara Orogen is more applicable to this discussion than Guj's (1967) work. Hälbich (1970) found that the Auas and Windhoek members of the Khomas Series display two co-axial fold systems (i.e. $B_1 // B_2$) and that the B_1 structures are represented everywhere in the Windhoek Member schists by a penetrative metamorphic banding cleavage. B_1 structures are present near Okahandja as the axial plane cleavage of upright B1 folds and are overprinted by a younger fracture cleavage which gains in intensity southwards until the older structures are refolded co-axially about B_2 axes. A transposition cleavage is developed in the schists of the Windhoek member where this B_2 deformation is most intense. Hälbich (1970) believes that wrench faulting and high angle thrusting mark the final surge of the Damara tectogenesis in the vicinity of the Auas Mountains, whereas a third fold phase, B_3, with associated fracture cleavage, essentially takes the place of this faulting in the Khomas Highlands.

Hälbich (1970) states that the three deformational phases were outlasted by biotite grade metamorphism and took place within a minimum time interval of 150 my.

At a much later stage, the Windhoek area was cut by a large number of subvertical tension fractures striking north-south. Subvolcanic material and breccia of trachytic composition ascended along these figures (Guj, 1967). Several volcanic necks and plugs were intruded in, and south of, the Auas Mountains at the same time.

3.2. Methods and Terminology

Twelve domains, homogeneous with respect to certain structural elements, were selected on and around Elisenheim for structural analysis (see Map 1).

A true statistical analysis was not carried out and the Schmidt net construction is used as a convenient way of representing the three-dimensionl fabric of the rock. Because most of the interpretation was done in the field, the Schmidt net diagrams must be considered semi-quantitative. The contoured synoptic diagrams confirm field observations and show that most of the elements are homogeneous throughout the area.

Contouring was undertaken according to the modified Schmidt method advocated by Guj (1970, p. 151-156). This method was chosen as it is most suitable for diagrams with large numbers of pointsor for diagrams with unusually high concentrations of points.

The magnetic declination for the Windhoek area during 1974 is taken as 21°.

There is much confusion about the terminology of most of the mesoscopic planes and linear elements in a fold system; this is mainly due to the fact that the genesis of these elements is not yet fully understood. To avoid this confusion and for practical reasons the system of Turner & Weiss (1963) will be used in this discussion. They advocate distinction of the different categories of planar surfaces observed in the field as s_1, s_2, s_3 ..... etc., followed by a list of the observable characteristics of each kind of s-plane. They catergorise lineations similarly and define lineation as those linear structures penetrative in handspecimens or in small exposures but treat larger scale linear features such as mullions, rods and elongate pebbles separately as linear structures. All the linear structures will, however, be treated, in this discussion, as lineations and will be described in the same manner as the planar structures.

Table 2. Notations of the various structural elements.

Fold phase	F_1	F_2	F_3
Bedding	ss	ss	ss
Bedding foliation	s_0	s_0	s_0
Fold axes	B_1	B_2	B_3
Foliation, schistosity and axial planes	s_1	s_2	s_3
b-lineation	l_1	l_2	l_3

3.2.1. Planar Structures

(a) Bedding (ss)

The uniformity of the schists and the transposed nature of the associated structures has prevented the identification of bedding within the Elisenheim schists. Bedding is recognisable north and south of the property where large scale changes in lithology occur.

(b) Bedding foliation (s_0)

Bedding foliation has not been recognised on Elisenheim. The small-scale, composition-banding folded about the prominent s_2-surface is axial planar to the earlier (B_1) folds of bedding near Okahandja in the north, and is definitely an s_1-surface. The small-scale and intricate folding of the bands and the repetitive occurrence of these layers, which do not have large lateral extensions, further suggest that this foliation was derived furing an earlier tectonic phase and does not represent bedding foliation.

(c) Foliation or Schistosity (s_1, s_2)

Most structures in the Windhoek area, especially in the more incompetent micaceous schists, have been appressed and sheared out leading to perfect examples of transposition foliation. Mesoscopic structures have, however, been preserved in the more competent quartzitic schists and it is from a study of these structures that a classification of the various planar and linear elements is derived.

s_1 is a metamorphic banding cleavage represented by alternating bands of more micaceous and more siliceous material (see plate 1) and near Okahandja is axial planar to B_1 folds. This foliation is folded about an axial-planar s_2-surface which formsa prominent, northwards-dipping cleavage surface. Both the s_1- and s_2-surfaces are recognisable within the quartzitic schists where they lie at low angles to one another but are indistinguishable in the micaceous "quartz-augen" schists where the folds have been obliterated and s_1-surfaces lie parallel to s_2.

It is impossible to differentiate between s_1 and s_2 stereographically because poles to these planes invariably plot within the same group and hinges of B_1 folds are highly appressed.

(d) Shear-cleavage (s_3)

In most of the micaceous schists and most of the fine-grained chloritic amphibole schists of the Matchless Amphibolite belt the s_2-schistosity is cut by closely-spaced planes (see plate 13) which are parallel to the axial planes of small crenulations. These north-trending and west-dipping s_3-surfaces mark the F_3 fold phase, kink the s_2-schistosity and form a wrinkle lineation, l_3, on it (Plate 11). Ramsay (1963) states that this cleavage is produced by the parting of the rock along zones where the micaceous minerals within the schistosity have been brought into parallelism on the fold limbs.

(e) Axial planes of folds (s_1, s_2 and s_3)

The orientation of the axial planes of the B_3 folds was measured wherever possible and was found to lie parallel to the s_3 shear-cleavage.

Schistosity and foliation both define planar structures and have the same meaning.

3.2.2. Lineations

(a) Fold axes (parallel to b-lineations l_2, l_3)

The direct measurement of B_2 fold hinges on mesoscopic structures was not always possible and measurements of this direction were taken from the quartz augen and rods of the schists. The augen plunge in various directions within the s_2-foliation and are believed by Hälbich (1970) to be detached and tightly closed fold hinges of F_2 age.

All l_3 measurements were taken on s_2-surfaces along the northwestwards plunging wrinkle lineation. These lineations represent the crests of minute crenulations (see plates 10 and 12) of F_3 age superimposed on s_2-surfaces. The s_3-shear cleavage is axial planar to these crenulations.

(b) Intersection Lineation (l_2)

The intersection of s_1- and s_2-foliation planes gives rise to a linear feature, l_2. This structure is common in the Elisenheim area but is only recognisable in the more competent quartzitic schists as alternating micaceous and siliceous lines trending east-west on s_2-cleavage surfaces (see plate 7). The bands plunge gently westwards parallel to B_2 axes.

Table 3. Fabric symbols used in stereographic diagrams.

Explanation	Symbol	
	Maxima of poles	Trace
s_1	●	– – – – – – –
s_2	●	–·–·–·–·–
s_3	●	–··–·–··–·–
π ss circle		— — —
πs_1 circle		— · — ·

3.3. Tectonic History

3.3.1. First Phase

Evidence of this phase is only present in fold closures of the more competent beds because in other lithologies in the area s_1 is essentially parallel to the later s_2 cleavage. A stereographic analysis of the relationships between ss and s_1 is also impossible since no horizons of original bedding are recognisable in the Elisenheim area. Discussion of the original orientation of s_1- surfaces and the extent of F_1 deformation

must therefore be directed to those undisturbed s-structures in the vicinity of Okahandja.

Hälbich (1970) in his synthesis of structures in the Windhoek-Okahandja profile states that this early phase of deformation is marked by a relatively undisturbed B_1 tectonite which outcrops from Okahandja to about 20 km south of the town. In a road cutting south of the Swakop River a succession of fine-grained biotite quartzites and quartzitic mica schists is thrown into nearly upright and slightly asymmetric open folds of intermediate size with wavelengths of tens to hundreds of metres. Axial surfaces and an axial plane metamorphic banding cleavage sf_1 (s_1 in this discussion) are parallel and vertical (see plate 1). Fold axes plunge at very low angles to the west. Hälbich (1970) believes that internal deformation, expressed as this cleavage, occurred early in the first phase of deformation and concomitantly with major folding.

The s_1-foliation occurs as innumerable fine lamellae one half to two millimetres wide, being alternatively more micaceous and more siliceous, in the schists, and as a fine fissility, no more than thin lines barely visible but one or more centimetres apart, in the quartzites. (Hälbich, 1970). This cleavage is accentuated by spindle-shaped metamorphic-segregation bodies which are aligned parallel to s_1 (see plate 1). Hälbich (1970) believes that these bodies have a segregational syntectonic origin and were formed during a prolonged period of regional amphibolite facies metamorphism that started just before or during the first phase of deformation and probably outlasted it. The spindles, which are more abundant in certain beds, have a preferred elongation near the regional B_1-axis.

The orientation of ss and s_1 in the country just south of Okahandja is expressed in the following two diagrams taken from Hälbich (1970, figs. 36 and 37).

Hälbich (1970) has found that the total symmetry of the system is monoclinic and that the B_1-axis plunges 10° southwestwards.

Further south of Okahandja a second phase of deformation is discernible and s_1 is folded about B_2 axes which lie in s_2 and are nearly or wholly co-axial with B_1 to the north. The intensity of the deformation of the B_1-structures increases southwards until, as in the Elisenheim area, transposition nearly obliterates the s_1-foliation. The occurrence of spindle-shaped metamorphic segregational bodies within the Elisenheim schists (termed granulite bands and lenticles by Hälbich, 1970), similar in size and mineral content to those present in the vicinity of Okahandja, further confirms the former presence of s_1-cleavage where transposition foliation is dominant.

The s_1-foliation is only present in the Elisenheim schists as a fine compositional layering in mesoscopic fold closures within the more competent quartzitic schists. s_1-surfaces are generally transposed parallel to s_2-surfaces in the incompetent micaceous schists and are not recognisable except when accompanied by spindle-shaped segregational bodies.

According to Hälbich (1970) the first phase of deformation is irrefutably manifested by refolded folds in bedding in the Auas Mountains.

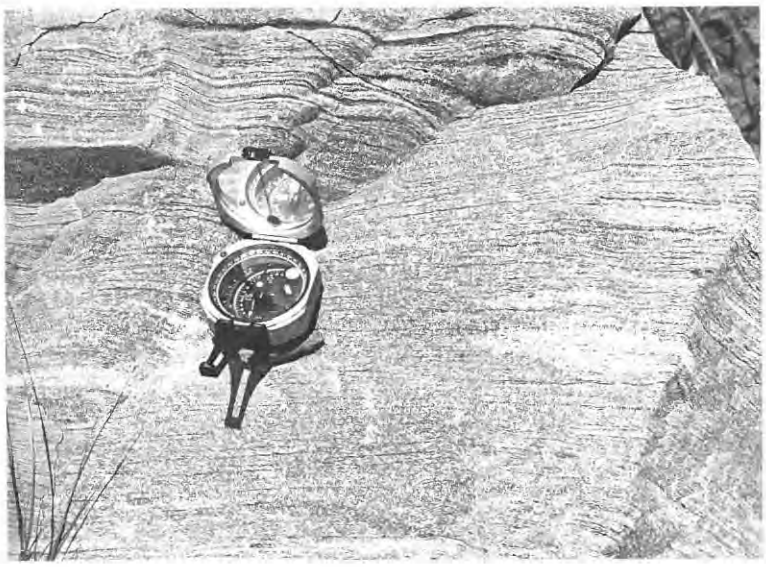

Plate 1. Steeply-northwards-dipping axial planar (metamorphic banding) cleavage s_1. Note the parallel orientation of spindle-shaped metamorphic segregational bodies (lighter coloured).

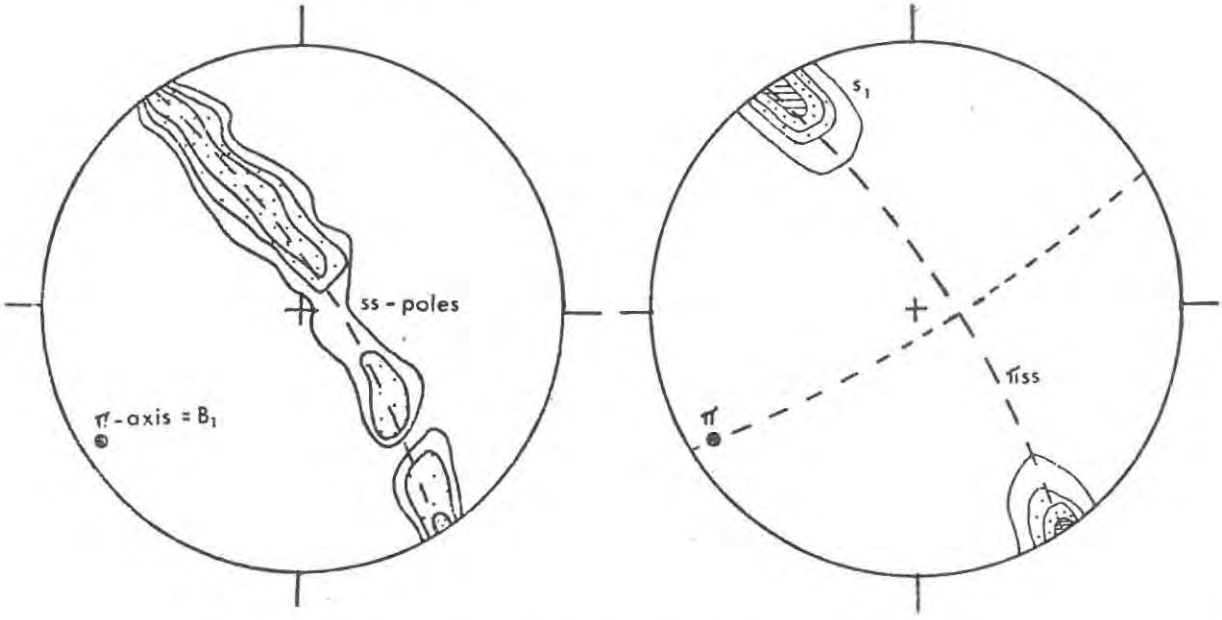

Figure 1. Structural data from the Okahandja area after Hälbich (1970, figs. 36 and 37).
(a) 82 poles to bedding (ss) fall on girdle along great circle ss. axis = B_1.
Contours at 2-5-10%
(b) 71 cleavage (s_1) poles plot on an elongated maximum.
Contours at 5-15-25-30%.

He states that the first phase folds in the Auas Range were overturned or became recumbent to the south before the second phase set in.

3.3.2. Second Phase

The country surrounding Elisenheim is characterised by structures of the F_2 phase of deformation. This phase is marked by a schistosity which dips northwards at about 30° and nearly obliterates the earlier s_1-foliation which is only preserved in the apices of folds in the more competent beds.

Hälbich (1970) in an attempt to determine the type, style and intensity of structures within the Windhoek stage of the Khomas Subgroup, undertook a systematic structural investigation at fairly regular intervals along the Eros escarpment between Okhandja and Windhoek. His interpretation of the structural evolution of the schists and quartzites will be presented as an introduction to the discussion of those structures observed in the Elisenheim area.

Deformation in the Okahandja area (see previous section) is marked by a relatively undisturbed B_1 tectonite which outcrops from Okahandja to about 20 km south of the town, from which point younger B_2 structures are discernible southwards. Hälbich (1970) states that this second phase is, at first, only expressed by a fairly steeply northwards-inclined cleavage, s_2, which is often locally inseparable from the earlier s_1-cleavage. Farther south (Hälbich, 1970, p. 115) s_2-cleavages and associated folds are superimposed, without notable effects of major second folding, upon the axial planar cleavage of open B_1 flexural-slip folds. This second phase is not quite co-axial with the first phase of deformation and Hälbich (1970) believes that oblique shear or non-affine slip may have occurred. In the vicinity of section 5 (Hälbich 1970, p. 116) the older s_1 cleavage is kinked about the younger cleavage which is almost parallel to bedding. The presence of an almost fully developed s_1 girdle (see Fig. 2) indicates, statistically, that on a larger scale s_1 is deformed.

The π-s_1 pole coincides exactly with the s_2/s_1 (B_2 axes) intersection and with the π-ss pole of sections 1-4 in the north (see Figs. 1(a) and 2). These facts prove that s_1 is folded about B_2 axes, which are nearly or wholly co-axial with B_1 and which lie in s_2.

About half way between Okahandja and Windhoek (Hälbich, 1970, p. 124) there is a fairly abrupt shallowing of the dip of s_2. Hälbich (1970, p. 153) continues thus:

"This change accompanies an intensification of the second deformation southwards as revealed by isoclinal and distinctly anisopach folds in bedding at first, that become almost completely appressed and sheared out in the Windhoek area, leading to a perfect example of transposition foliation".

Transposition (foliation) is best developed in the incompetent micaceous quartz augen schists where all s-surfaces are parallel and the only confirmation of the former presence of s_1-surfaces is exhibited by the quartz augen. Close study (see plate 4) of these augen and the thin layers of micaceous quartzite shows that many of the augen are

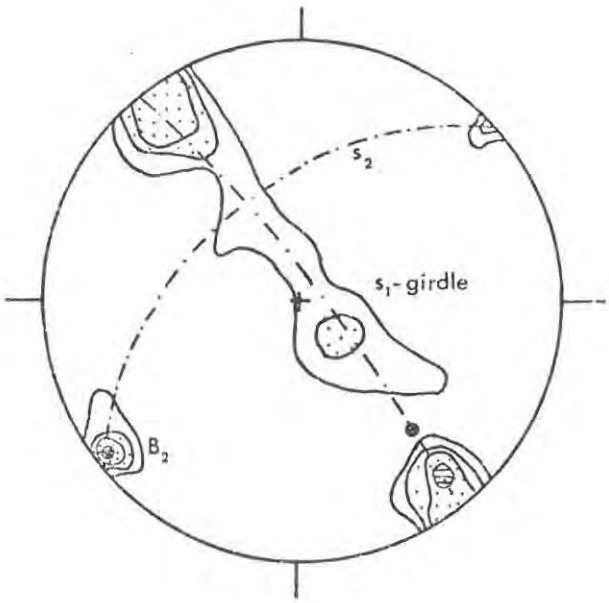

Figure 2. Structural data from section 5, Hälbich (1970, p. 116).
50 poles to cleavage (s_1).
Contours at 2-5-10-20%.
21 B_2 axes. Contours at 20-40-60%.

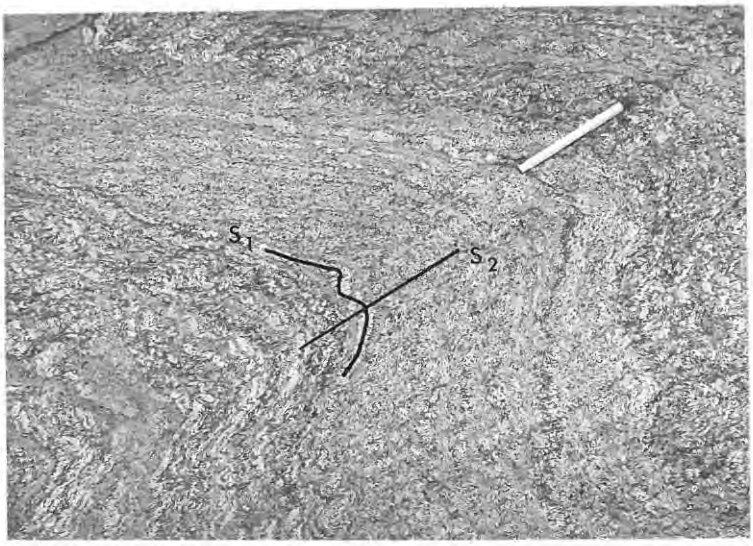

Plate 2. Otjihavera Gorge (section 9). An example of the intensification of the folding of s_1 and the development of an s_2 axial planar cleavage.

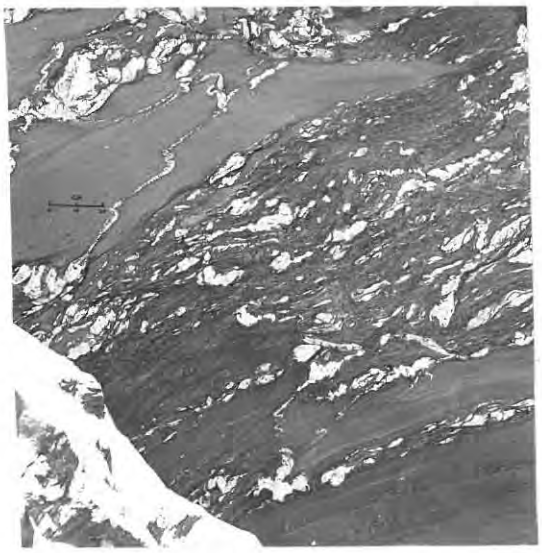

Plate 3. An upper band of competent quartzitic schist with a lower unit of incompetent micaceous quartz-augen schist (displaying transposition foliation, quartz augen).

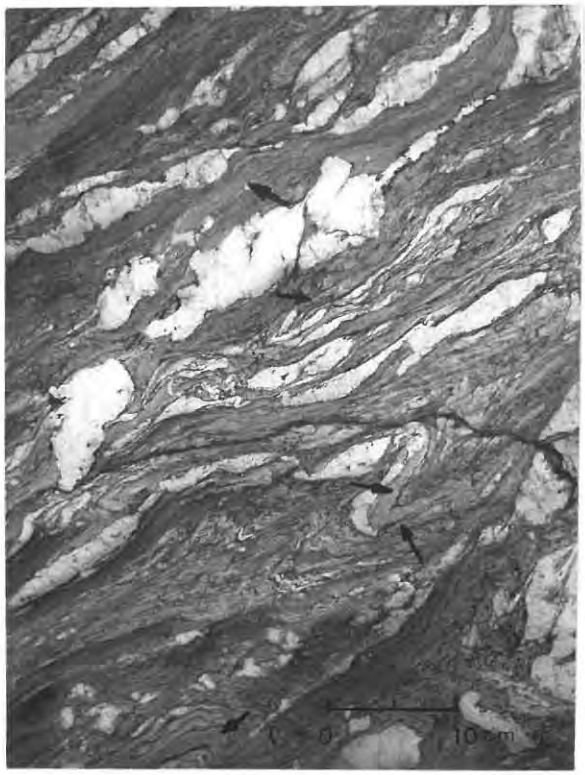

Plate 4. Incompetent micaceous quartz-augen schist with fold hinges (B_2) indicated by quartz augen and quartz-schist (arrows).

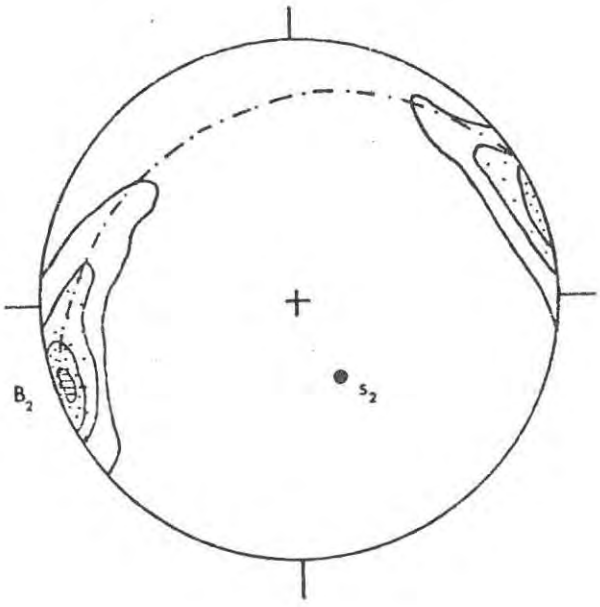

Figure 3. Structural data from Elisenheim.
78 quartz vein fold axes. Contoured at 1-3-7-10%.

Plate 5. s_1 surfaces preserved in competent quartzitic schist.

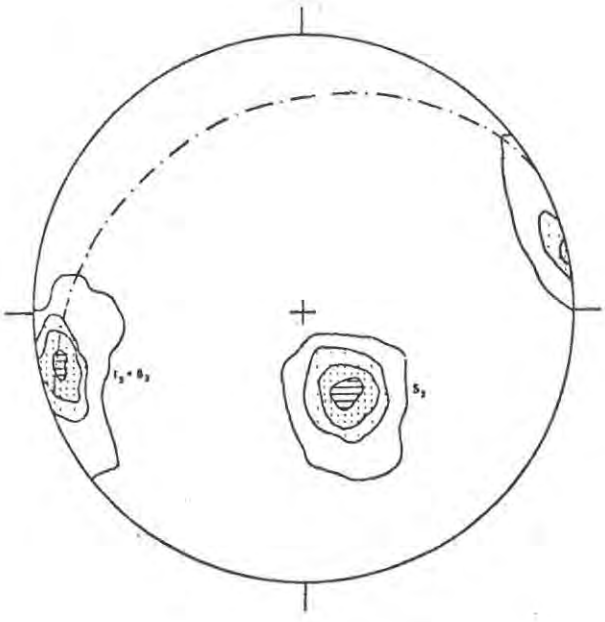

Figure 4. Structural data from Elisenheim.
277 poles to schistosity (s_2) contoured at 1-10-30-50%.
225 intersection lineations (l_2) contoured at 1-20-40-60%.

detached and tightly-closed fold hinges.

Rodding due to the intersection of the quartz veins and the s_2-schistosity is very common. There has been some doubt as to whether these quartz-augen represent disrupted quartz veins of an earlier (B_1) age or whether they formed during the later (B_2) stage. Hälbich (1970) believes that the quartz veins folded in this area belong to the same generation as those not yet folded in the north and that the quartz-augen of the Elisenheim area developed from the deformation of B_1-stage quartz veins. For these reasons the quartz veins are the key to an analysis of those structures of the Elisenheim area where s_1 and s_2 surfaces generally parallel to each other.

A plot of the quartz vein fold axes indicates a distribution along a girdle parallel to the trace of s_2 with a maximum near the B_2 fold axis (see Fig. 3). This lineation is dispersed symmetrically about the B_2 fold axis direction, within the schistosity, and is pre-B_2 as it was folded during F_2 deformation.

Mesoscopic folding of s_1-surfaces can be recognised in competent beds (usually fine-grained micaceous quartzites and quartzitic schists). These folds depict the style of folding prevailing in this area and possibly reflect the behaviour of competent beds on a larger scale. s_1-surfaces that are not transposed into s_2 are not commonly found and most outcrops display the dominant northwards dipping s_2-foliation (see Plate 6 and Figure 4).

Figure 4 shows that s_2 strikes at N61°E and dips at 27° northwards.

An intersection lineation, l_2, (Plate 7) the characteristics of which were described in 3.2.2. (b) plots with a maximum near the B_2 axis and plunges at 10° on 258°.

The symmetry of the system is orthorhombic (i.e. that of a plane with a lineation in it) despite the fact that the quartz vein fold axes do not fall within a single maxima in the direction of the B_2 fold axis.

Second phase isoclinal folding and transposition have destroyed all original bedding relationships within the schists, individual lithologic units do not persevere for great distances along strike and contacts between the various beds are transposed. These transposition effects are also noticeable in the Matchless Amphibolite belt.

Structures resembling pillows are present within bands of epidote amphibolite on Elisenheim. Similar structures reported at Matchless Mine have been interpreted as evidence of basic volcanicity (M.J. Viljoen quoted in Anhausser and Button, 1974, p. 23). Field and petrographic studies have shown that these bodies are not pillows but represent boudinage structures formed during the Damara tectonism. These conclusions have been confirmed by Krõner (1974, p. 180) who clearly proves that the "sausage-shaped" bodies formed by differential movement of competent and incompetent layers within the regional foliation. The boudins exhibit none of the features typical of pillow lavas and are elongated parallel to the b-lineation, l_2. The structures are arranged in typical boundinage fashion, similar to the quartz augen, within the regional foliation. Reference to Plates 8 and 9 will show that "cores" of massive epidote amphibolite are surrounded by "selvedges" of

Plate 6. Typical Khomas schist with northwards dipping s_2.

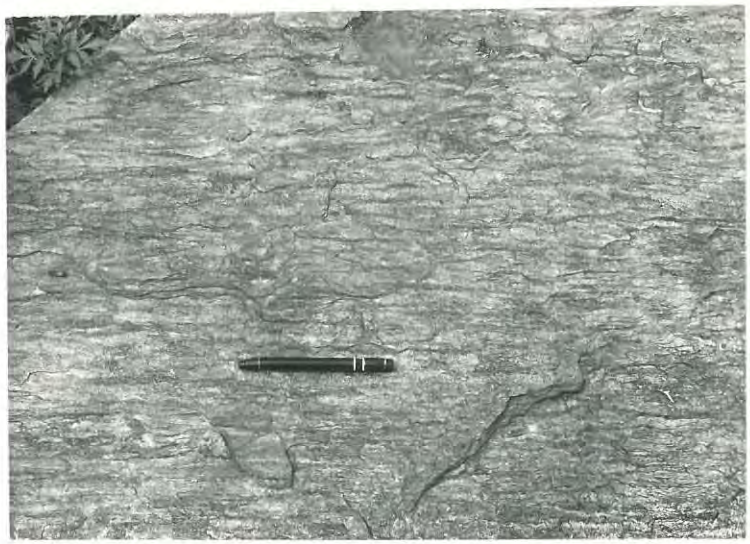

Plate 7. Westward plunging l_2 intersection lineation parallel to rapidograph.

sheared quartzitic schist, which probably reflect the breakup of once continuous competent 19-15 cm thick bands of amphibolite sandwiched between less competent quartzitic layers (Krõner, 1974, p. 178).

3.3.3. Third Phase

Hälbich (1970) states that a north-trending, west-dipping s_3 fracture cleavage, which kinks the schistosity and forms a wrinkle lineation on it, is present at localities west of Windhoek. He believes that this cleavage is not a penetrative structure like s_2 in the zone of transposition, but develops sporadically only to fade again. Furthermore, Hälbich (1970) notes that the Aretaragas Fault, which lies a few kilometres west of Windhoek and trends north-south, forms the abrupt eastern boundary of the area of distribution of the s_3-cleavage.

Contrary to Hälbich's (1970) findings, field work has shown that this s_3-fracture cleavage and associated l_3 wrinkle-lineation is well-developed east of the Aretaragas Fault at least as far as Otjihase Mine, the easternmost limit of the area mapped by the author.

The wrinkle lineation is most often recognised on s_2 schistosity surfaces of the more micaceous schists of the area and is commonly observed as shown in Plate 10. Kinking of the s_2-surfaces accompanied by the production of a prominent l_3 lineation, is best developed in the incompetent chloritic amphibole schists and talc schists of the Matchless Amphibolite belt. The kinks usually have a crest-to-crest distance of 0,5 cm to 2,5 cm except in the talc schists of northwestern Elisenheim, where the wavelength of the folds is approximately 0,3 m. No major s_3-structures are developed. Typical examples of crenulations and l_3 lineation within incompetent amphibolitic schists are shown in Plates 11 and 12.

The best examples of the s_3 shear cleavage are found in the competent quartzites near Matchless Mine. The cleavage which is shown in Plate 13, cuts across the schistosity and dips westwards. Due to the competent nature of the beds it is developed at the expense of the microfolds and is refracted when it passes through layers of differing competency.

The structural elements of the third phase of deformation are plotted in Figure 5. The s_3 shear cleavage dips westwards at 44° and the lineation plunges at 29° on 322°.

The maximum of the l_3 crenulations plots at the intersection of the s_2- and s_3-surfaces and is the direction of the B_3 fold axis since (i) this position lies within the axial plane and (ii) the lineation measured represents the hinge-line of the crenulations. The s_3-cleavage is axial planar to the crenulations.

The crenulations, when studied in handspecimen, appear to possess curvilinear hinges (lying in a plane) and to be planar non-cylindrical folds. Statistical analysis, however, shows that hinges are rectilinear on a macroscopic scale and that the crenulations are plane cylindrical folds of s_2-surfaces, despite the fact that they have been superimposed on already folded surfaces. The symmetry of the system consists of a s_3-plane with a lineation in it and is orthorhombic.

Plate 8

Plate 9. Boudins of massive epidote amphibolite rimmed by quartzitic schist with quartz fillings in fractures and at "tail-edges" of boudins, Elisenheim 68.

Plate 10. Typical l_3 wrinkle-lineation on s_2-schistosity in Khomas schists, Elisenheim 68.

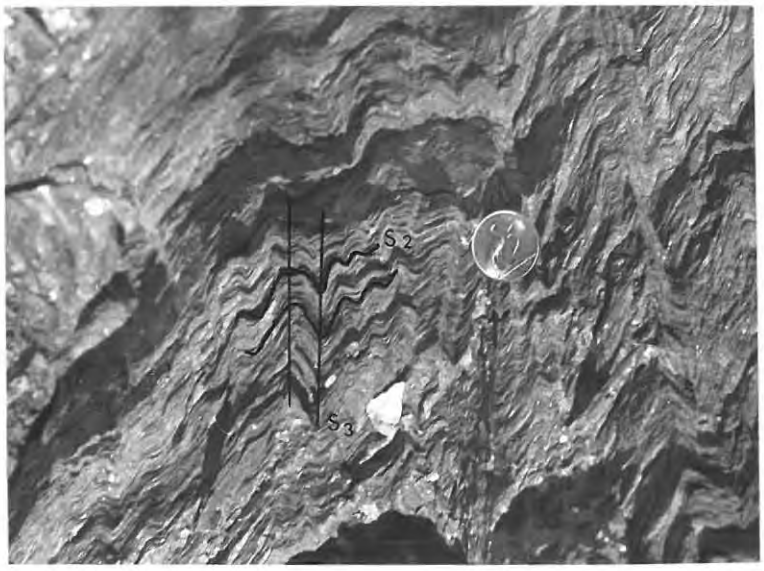

Plate 11. Small-scale folding of s_2-surfaces, and s_3 shear cleavage in chlorite amphibole schist, Matchless Amphibolite, Elisenheim 68.

Plate 12. Northwest-plunging l_3 lineation in talc schists, Elisenheim 68.

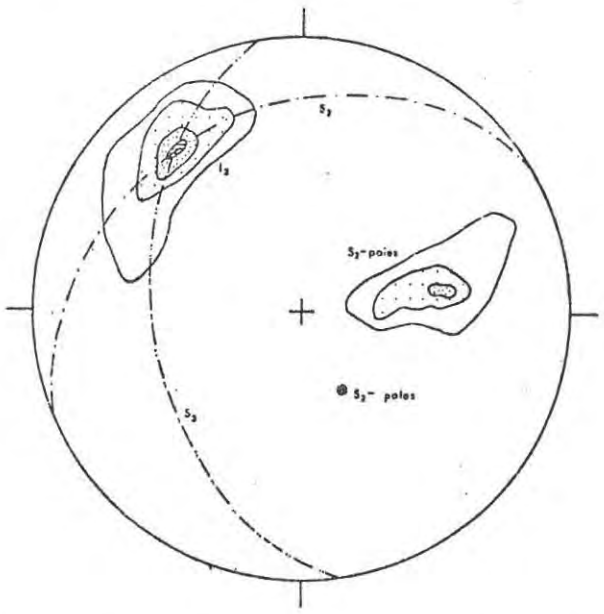

Figure 5. Structural data from Elisenheim and Matchless Mine. 113 lineations (l_3) contoured at 1-10-30-40%.
56 poles to shear cleavage (s_3) contoured at 2-10-20%.
s_2 poles from Figure 4.

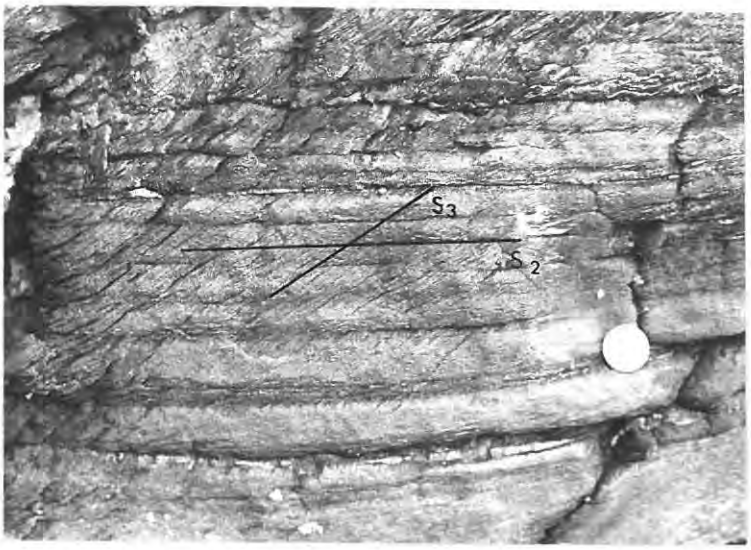

Plate 13. West-dipping s_3 shear cleavage developed in sericitic quartzite near Matchless Mine.

3.3.4. Faulting

Three large north-south trending and sub-vertical faults transect the schists and amphibolites underlying Elisenheim and are recognisable on aerial photographs as north-south trending river beds. The westernmost of these faults underlies the Klein Windhoek River (Pahl Fault of Hälbich, 1970) and forms the eastern boundary of the Windhoek valley. The Windhoek valley is an erosion feature along a north-south trending zone, 10 kilometres wide, of closely spaced breccias (Gevers, 1934) which is bounded by two step faults down-thrown to the west. The other two faults on Elisenheim underlie the Dõbra and Tigenschlucht Rivers. These rivers cut deep gorges through the terrain and the fault planes are present as steeply westward-dipping zones of ferruginous and siliceous mylonite (see Plate 4). The mylonite zones are generally brecciated and are accompanied by zones of small fractures which lie on either side of the fault and run parallel to it.

Brecciation of the mylonite indicates that a number of episodes of faulting occurred. Early intense downthrow which caused the development of the mylonite was possibly followed by a period of less intense settling which fractured the mylonite.

The orientation of sets of slickensides in the fault planes suggests vertical movement although it is realised that total displacement along a fault may be the sum of several individual movements in different directions of which only the final surge is revealed by slickensides. Hälbich (1970), however, states that the orientation of slickensides (and pebble lineations) on these fault planes, even if they only reflect the final movements, is still in agreement with a stress distribution that readily accounts for the B_2 fold phase as well.

Plate 14. West-dipping mylonite zone at southern end of Dõbra River fault, viewed from the north.

Guj (1967) states that the northern extensions of the faults in the Auas Mountains are normal faults. Consequently if the faults on Elisenheim are similar no lateral component of movement need be present; however, no vertical or steeply-dipping structures have been faulted to substantiate such a conclusion. Studies on faults at Otjihase Mine (Anonymous, 1973) indicate that all faults are normal and downthrown to the west and it is assumed that the Elisenheim faults are similar in style.

Reference to the geological plan will show that all units of the Matchless Amphibolite are apparently displaced by about 1500 m. This step-like faulting of the Matchless Amphibolite accounts for its presence just north of Otjihase Mine. Evidence of faulting west of the mine is present as ferrugenous mylonite lying in the north-south trending Otjihase river bed.

The faults lying between the Klein Windhoek (Pahl Fault) and Otjihase rivers do not develop any hinge effects since all lithological units are displaced a similar distance horizontally, although Hälbich

(1970) found a northwards-increasing hinge effect along the Aretaragas Fault (which lies a few kilometres west of the area investigated by the present author). By analogy, he postulates that the Pahl Fault rapidly develops a hinge effect south of Windhoek and, immediately north of Windhoek, offsets the Matchless Amphibolite northwards in the east far beyond the area covered in his investigation. This is incorrect as units of the Matchless Amphibolite are only offset by 1500 metres and, due to the width of outcrop of the belt, virtually overlap on both sides of the fault.

The amphibolite belt narrows down west of the Pahl Fault to three main units, each with a maximum thickness of 100 metres, spread over an outcrop width of 1500 metres. It is most probable that the difficult identification on aerial photographs of such a relatively narrow belt of rocks in mountainous terrain has prompted Hälbich (1970) to believe that these units are not present east of the Pahl Fault immediately north of Windhoek and so postulate a hinge component for the Pahl Fault.

Guj (1967) has concluded that faulting and folding occurred contemporaneously. This is confirmed by Hälbich (1970) who believes that bending of the regional Damara fold trend around the Hohewarte Gneiss Complex and its northward continuation underneath the Damara System was responsible for locating a zone along which faulting and the s_3-cleavage developed as a final expression of the regional stress configuration. He states that a genetic relationship between faulting and the s_3-cleavage is present and that wrenching and thrusting around Windhoek and in the Auas Mountains occurred late during the B_2 phase. Hälbich (1970) therefore concludes that the Aretaragas and similar faults compensated for any residual strains set up by basement irregularities in the Windhoek area but that west of the Aretaragas Fault this was achieved mainly by shear folding and cleavage in addition to minor faulting. The presence of s_3-cleavages east of the Aretaragas Fault throughout the Windhoek area somewhat invalidates the above conclusion. This coupled with the lack of hinge faulting in the Elisenheim area has caused the writer to favour Guj's (1967) interpretation.

At a much later stage the whole area was cut by a large number of north-south striking tension fractures along which subvolcanic and trachytic breccia material was emplaced. The presence of trachytic material within fault-planes of Damaran age is explained (Guj, 1967) by the fact that these brecciated and mylonitised rocks behaved as lines of weakness along which uprising material was emplaced during a phase of rejuvenation.

3.4. Summary

The strata underlying Elisenheim display three phases of tectonic deformation. The earliest structures are preserved as a metamorphic banding cleavage, which lies either at very acute angles to the s_2-foliation, or as very tightly appressed mesoscopic folds. According to Hälbich (1970) these B_1 structures are present to the north as major and minor upright folds. Overprinting by a younger s_2 fracture cleavage intensified southwards until the older structures were refolded co-axially during the B_2 phase. Increased deformation in the Windhoek area resulted in the obliteration of earlier structures in the schists and the development of a transposition s_2-foliation. Countless quartz-augen and

rods are present in the more incompetent transposed micaceous schists and are believed to represent detached and tightly closed fold hinges of B_2 age. The dominant s_2 foliation dips northwestwards at 30°. A west-dipping, north-trending s_3 shear cleavage and associated crenulations kink the s_2-schistosity and form a l_3 wrinkle lineation on it, plunging northwestwards at 30°. A genetic relationship between the B_2 folding and the development of the major north-south trending faults has been established by Guj (1967) and Hälbich (1970). It is probable that the faults and s_3-cleavage developed contemporaneously.

Hälbich's (1970) supposition that the major north-trending faults compensated for any residual strains set up by basement irregularities in the Windhoek area and that west of the Aretaragas Fault this was achieved mainly by shear folding and cleavage in addition to minor faulting, is somewhat invalidated by the presence of shear folding and cleavage in the Windhoek area. It is likely that the strains set up by basement irregularities in the Windhoek area were greater than elsewhere and that this resulted in major faulting besides the development of a shear cleavage.

The presence of these many fractures has influenced the location of the numerous post-Damara trachytic and phonolitic plugs and dykes observed in the Windhoek district. Volcanic activity during Jurassic times (Hälbich, 1970) reactivated these Damara faults besides producing a large number of subvertical tension fractures along which subvolcanic material and breccia, mainly of trachytic composition (Guj, 1967), ascended.

All units of the Matchless Amphibolite belt have undergone the three phases of deformation and it is likely that the braided appearance of the belt is due to transposition of multiple flows or intrusions.

4. PETROGRAPHY AND METAMORPHISM

A total of 97 thin sections was studied under the microscope. This investigation shows that the mineral assemblages in the rocks are similar to those of the amphibolite facies (Turner, 1968) and that the metamorphic grade is constant throughout the area.

For the purposes of description and interpretation the rocks have been assigned to three compositional categories, semi-pelitic, basic and ultrabasic.

4.1. Semi-pelitic Association

4.1.1. Petrography

Reference to the geological plan will show that Khomas schists form the bulk of the rocks underlying the Elisenheim area. These schists are characterised by a prominent northwards-dipping transposition foliation which has obliterated all original bedding and resulted in the formation of an undifferentiated mass of quartz biotite schist and micaceous "quartz-augen" schist (see Plate 3).

The mineral assemblages encountered in the quartz-biotite schists are as follows:

(a) quartz-biotite-potassium feldspar-epidote-muscovite-plagioclase-chlorite-magnetite-apatite.

(b) quartz-biotite-potassium feldspar-epidote-muscovite-plagioclase-chlorite-magnetite-garnet.

(c) quartz-biotite-potassium feldspar-chlorite-magnetite-plagioclase-garnet.

The quartz biotite schists are characterised by flakes of biotite and minor amounts of associated muscovite and chlorite aligned parallel with the s_2-foliation surface and set in a mosaic of clear, xenoblastic quartz grains averaging 0.1 mm to 0.2 mm in size. Minor amounts of granular epidote are present along with traces of ore, euhedral to subhedral apatite and green tourmaline. The estimated modal composition of a typical quartz schist is shown in Table 4.

Accurate estimates of the total thin section or handspecimen mineralogical content of samples of micaceous "quartz-augen" schist are difficult to make since much quartz is concentrated in the augen which are often elongated parallel to the l_2-lineation and are irregularly scattered throughout the micaceous schists. Only sampling of a very large surface area, far beyond the scope of micrometric analysis, will give a true reflection of the modal composition. The modal composition of SF78 (see Table 4) was obtained from a combination of visual and micrometric estimates.

The bulk of the schistose material consists of alternating bands, 1 mm to 3 mm wide, of interlocking quartz grains and micaceous minerals. The quartz grains form xenoblastic mosaics whereas the micas outline B_3 folds and kinks (Plate 15); large biotite flakes have grown across

Table 4. Estimated modal compositions in volume percent of two typical Khomas schists

Mineral	Quartz-biotite schist SF79	Micaceous "quartz-augen" schist SF78
Quartz	53	45
Biotite	29	15
K-feldspar	7	-
Epidote	6	1
Muscovite	4	25
Chlorite		12
Magnetite	1	1
Apatite	1	tr
Garnet	tr	1
Tourmaline	tr	-

this schistosity indicating that biotite metamorphism has outlasted deformation. The micaceous minerals predominate and make up most of the inter-"quartz-augen" schistose material. Occasional idioblastic to sub-idioblastic garnet porphyroblasts have grown in chlorite-amphibole partings across the s_3 foliation which indicates that garnet metamorphism outlasted deformation. Grains are usually fractured and weathered but refractive index determinations on rare fresh grains gave values between n = 1.780 and n = 1.800. In the absence of data on the specific gravity and cell-edges of the grains it was not possible to determine the content of the garnets in terms of three- or four-component composition fields. The garnets, however, are probably almandine-rich and are typical of

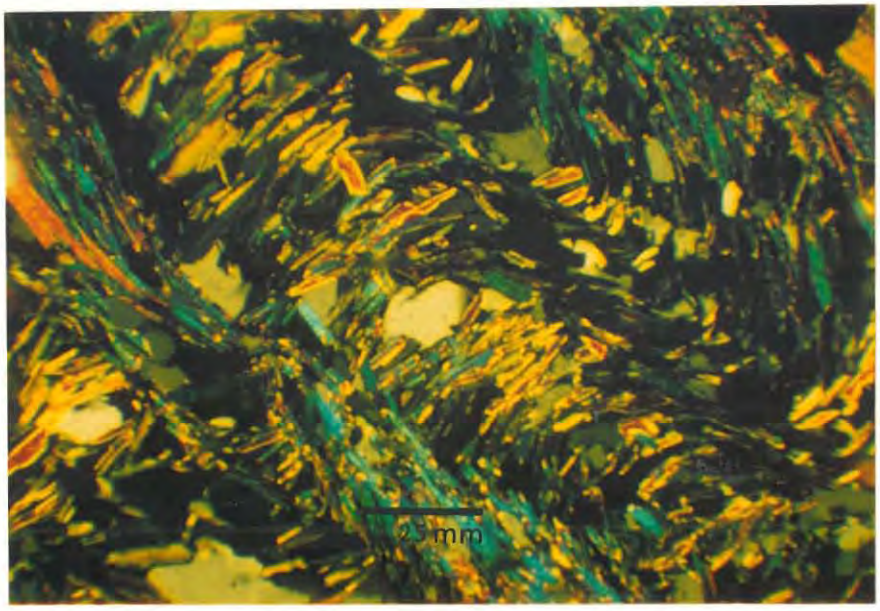

Plate 15. B_3 folds in micaceous "quart-augen" schist.

garnetiferous schists resulting from the regional metamorphism of argillaceous sediments.

The mineral assemblages typical of the micaceous "quartz-augen" schists are as follows:

(a) quartz-muscovite-biotite-plagioclase-chlorite-magnetite-garnet-epidote

(b) quartz-chlorite-muscovite-biotite-potassium feldspar-magnetite-garnet-plagioclase-epidote

Samples SF78 and SF79 are typical, mineralogically and texturally, of the Khomas schists of the Windhoek area. The mineralogical differences are reflected in the chemistry of these rocks which is presented in Table 5. Sample SF79, which contains more modal quartz and less mica than SF78, is enriched in SiO_2 relative to SF78 and depleted in Al_2O_3, FeO, MgO and total H_2O. Reference to Figure 7 shows that these Khomas schists plot adjacent to the fields of pelites and semi-pelites.

Table 5. Chemical analyses, in weight percent of oxides, of 2 Khomas schists, and a typical pelitic mica schist.

Oxide	* SF78	* SF79	+ Mica schist
SiO_2	61,48	72,53	60,42
TiO_2	0,94	0,73	0,91
Al_2O_3	15,42	12,19	16,41
Fe_2O_3	0,77	1,29	2,85
FeO	5,92	3,32	6,84
MnO	0,16	0,08	0,09
MgO	4,47	1,68	3,76
CaO	2,20	1,99	0,96
Na_2O	1,33	2,76	1,60
K_2O	3,11	2,23	3,25
P_2O_5	0,10	0,08	0,21
H_2O^+	2,27	0,93	2,39
H_2O^-	0,08	0,04	
CO_2	1,11	0,05	
Total	99,36	99,90	99,69
Cr	140 ppm	73 ppm	
Co	38 ppm	23 ppm	
Ni	42 ppm	30 ppm	

* Analyses by General Superintendence Co.
\+ After Mehnert (1969, p. 278).

Narrow (< 2 m) bands and lenses of graphitic schist, ferruginous quartzite and actinolite schist outcrop infrequently within the semi-pelitic schists. The carbonaceous horizon is black in handspecimen and extremely fine-grained with individual grains not recogniseable under high power. B_3 minor folds are common (see Plate 16). The ferrugineous quartzite which outcrops west of Elisenheim is characterised by a granuloblastic texture with quartz grains ranging in size from 0.1 mm to 1 mm. Quartz is the dominant mineral and accounts for about 80% of the thin section studied. The opaque minerals, mainly magnetite and oxidised sulphides constitute 17% of the specimen and occur as xenoblastic grains lying at or near the triple point intersections of the quartz grains and are arranged in sub-parallel and parallel (to S_2) bands across the rock. Minor amounts of pleochroic green chlorite, brown biotite and carbonate are occasionally associated with the magnetite. Less than 1% anhedral apatite is also present. Fractures filled with ferrugineous material resulting from oxidation of magnetite and sulphides give the rock a "gossanous" appearance.

Sericitic quartzite, similar to units outcropping adjacent to the amphibolite belt in the Matchless Mine area, were not found on Elisenheim. Coarse-grained, sugary, white quartz veins are common within the Khomas schists of Elisenheim.

Plate 16. F_3 folds in graphitic schist. Plane-polarised light, SF12.

4.1.2. Discussion

The mineral assemblages of the Elisenheim rocks are compatible with those of the amphibolite facies (Turner, 1968) but are not indicative of the grade of metamorphism since they contain no index minerals besides almandine garnet.

Winkler, (1974) has divided the entire P, T range of metamorphic conditions into four large divisions of metamorphic grade:

namely, very-low grade, low grade, medium grade, high grade, the boundaries between which are marked by significant metamorphic changes of mineral assemblages in common rocks. The reactions for boundaries between metamorphic grades have been selected to reflect changes that take place at the beginning of the greenschist facies and at the beginning of the amphibolite facies, respectively. Thus the boundary between "very-low grade" and "low grade" coincides with the beginning of the greenschist facies and the boundary between "low grade" and "medium grade" coincides with the beginning of the amphibolite facies of Eskola.

The first formation of cordierite and/or staurolite in pelitic rocks of appropriate composition is defined by Winkler (1974, p. 234) as the beginning of medium-grade metamorphism. The most common reactions producing these minerals are probably the following:

(1) chlorite + muscovite + quartz = cordierite + biotite + Al_2SiO_5 + H_2O

In order to form staurolite, chlorite containing an appreciable amount of ferrous iron is needed (Winkler, 1974, p. 76).

(2) chlorite + muscovite = staurolite + biotite + quartz + H_2O.

Work by Puhan and Hoffer (1973) indicates that the first appearance of staurolite, closely followed by the appearance of kyanite as the stable modification of Al_2SiO_5 in pelitic rocks, occurs in an area 60 km southeast of Elisenheim. Staurolite most probably formed by reaction (2). This reaction indicates the beginning of Winkler's (1974) zone of medium grade metamorphism and is illustrated in terms of P,T conditions in Figure 6. The close appearance of staurolite and kyanite in Puhan and Hoffer's (1973) area suggests that the Elisenheim semi-pelites, which lie higher up in the Khomas stratigraphic succession and are higher in terms of metamorphic grade, locate to the higher temperature side of reaction (2).

Winkler (1974, p. 81) has defined the boundary of medium to high grade as the breakdown of muscovite in the presence of quartz and plagioclase which takes place by the reaction:

(3) muscovite + quartz = K-feldspar + Al_2SiO_5 + H_2O.

The presence of prograde muscovite within the Elisenheim semi-pelites suggests that this reaction has not yet begun and that the semi-pelites are siguated below the medium to high grade boundary. This is true as reaction (2) only takes place to the WNW of Elisenheim nearer to the central part of the belt.

It is evident from the work of Martin (1965, p. 41) that Elisenheim lies south of the occurrence of andalusite and sillimanite which are common in the pegmatite zone which accompanies the granitised and granite-invaded belt of the orogen. Investigations by Jacob (1974, p. 129) east of the confluence of the Khan and Swakop rivers has confirmed the inversion of andalusite to sillimanite within the granitised zone (as in reaction (4)):

(4) andalusite = sillimanite

The disappearance of andalusite is accompanied by the decomposition of staurolite in pelitic rocks (Jacob, 1974, p. 126):

(5) staurolite + muscovite + quartz = biotite + almandine + Al_2SiO_5 + H_2O

This reaction (5) takes place at slightly higher pressures than (6) (Winkler, 1974, p. 217) which, along with reaction (4), defines the possible upper limit of metamorphic grade for the Elisenheim area:

(6) staurolite + muscovite + quartz = Al_2SiO_5 + biotite + H_2O

It is clear from the aforegoing discussion that the Elisenheim area lies geographically just south of midway between the appearance of staurolite (2) and kyanite, on the one hand, and the disappearance of staurolite (6) and the inversion of andalusite to sillimanite (4) on the other hand. The temperature conditions prevailing during metamorphism of the Elisenheim rocks should therefore plot about midway between reactions (2) and (4) and (6) i.e. in the vicinity of the kyanite to sillimanite inversion line. Puhan and Hoffer (1973, p. 213) have estimated that the minimum pressure conditions prevailing during the metamorphism of their area southeast of Elisenheim were 5 kb. This suggests that pressure conditions were above 5 kb but below the pressure defined by the triple point because andalusite and sillimanite occur north of the property. The conditions of metamorphism operative in the Elisenheim area should therefore fall in the stipled area (see Fig. 6) if temperatures of 550°C to 600°C are assumed (Puhan and Hoffer, 1973).

The positioning of the Elisenheim semi-pelites within Winkler's (1974) zone of medium grade metamorphism is valid despite the presence of prograde muscovite plus chlorite, which, with the exception of a small range of co-existence, should be absent in medium grade rocks. It is probable that the Elisenheim rocks lie just beyond the "staurolite-in" isograd but that the chlorites are Mg- rather than Fe-rich. This would preclude the formation of staurolite (Winkler, 1974, p. 76) and allow for the presence of (Mg-) chlorite which is stable at higher temperatures than its Fe-rich counter-part. This supposition is confirmed by thin section studies which indicate that the chlorite present is prochlorite.

Minor amounts of granular epidote coexist with quartz. This indicates that the reaction

(7) epidote + quartz = anorthite + grandite + haematite + H_2O

determined by Nitsch and Winkler (reported in Jacob, 1974) has not yet taken place. A further indication of the operative metamorphic conditions is given by the positioning of this reaction curve (7) in Figure 6.

The frequent growth of large biotite flakes and occasional garnets across the foliation indicates that garnet and biotite metamorphism has outlasted F_3 deformation.

4.2. Basic Association

Petrographic studies on amphibolite samples collected from the Elisenheim area and Matchless Mine have resulted in the recognition of three types of amphibolite, namely, chlorite-amphibole schist, porphyroblastic amphibolite and epidote amphibolite. Chemical evidence

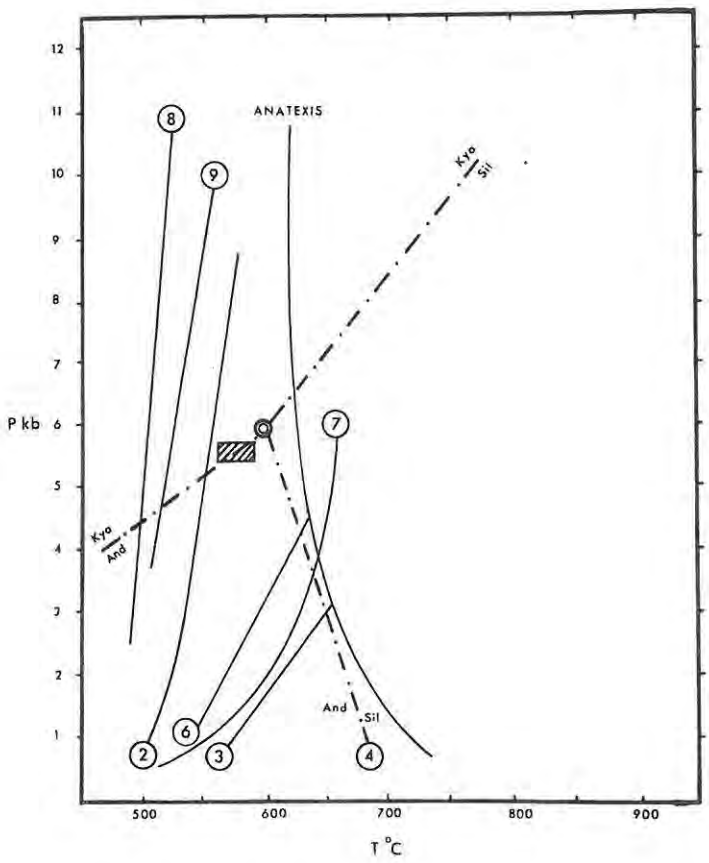

Figure 6. P-T diagram showing experimentally determined equilibrium curves for reactions discussed in text. Figures in brackets refer to reactions cited and the hatched area indicates probable P-T conditions in the Elisenheim area.

(2) mus + chl = stt (Winkler, 1974, p. 234)
(3) mus + qz = ksp + Al_2SiO_5 + H_2O (Winkler, 1974, p. 236)
(6) stt + mus + qz = bio + Al_2SiO_5 (Winkler, 1974, p. 236)
(7) Epid + qz = an + gran + haem + H_2O (see text)
(8) Hbl-in ; Alm (Winkler, 1974, p. 232)
(9) An_{17} + Hbl (Winkler, 1974, p. 232)
Al_2SiO_5 polymorphs (Winkler, 1974, p. 236).

(see Chapter 5) suggests that these units and the talc schists are genetically related.

4.2.1. Chlorite-amphibole schist

This rock-type is, chemically, the most basic of the three amphibolites and usually outcrops as a fine-grained, highly crenulated, dark green schist (see Plate 11). Thin section studies indicate that samples are typically schistose with hornblende grains (0.1 mm to 0.5 mm in length) and chlorite flakes aligned parallel to the F_2 schistosity. These grains are kinked by B_3 crenulations which indicates that growth took place before the F_3 phase of deformation. Occasional hornblende grains have grown parallel to the axial planes of the F_3 crenulations but many needles are randomly orientated indicating minor post-B_3 growth of hornblende.

The modal content of SF77, a typical chlorite-amphibole schist is presented in Table 7. The mineral assemblages of typical chlorite-amphibole schists are as follows:

(a) Hornblende-actinolite-plagioclase-chlorite-epidote-biotite-quartz-magnetite

(b) Hornblende-actinolite-chlorite-plagioclase-epidote-calcite-quartz

The hornblende grains show occasional patchy zoning of actinolite. This phenomena is more pronounced in the porphyroblastic amphibolites and is discussed fully in section 4.2.4. The chlorite grains are light green and pleochroic and have a low birefringence. Biotites are brown, strongly pleochroic and up to 1 mm in length. The smaller biotite grains often occur in association with magnetite and define the dominant schistosity whereas growth of large porphyroblasts appears to have outlasted deformation as these grains cut across the s_3 foliation. Granular epidote grains with bluish-yellow interference colours, are <0.1 mm in size and are more commonly found associated with quartz. Plagioclase feldspar grains are generally ~0.1 mm in size with some grains displaying zoning. The zoning is indistinct and the recognition of zones is virtually impossible. Universal stage determinations of anorthite content show that the rims are more calcic (An_{30}) than the cores (An_{0-10}) which is indicative of prograde metamorphism. Strain effects are noticeable in the occasional quartz grains and this effect sometimes obscures zonal structures in the plagioclases. Accessory sphene is present and usually occurs in close association with ilmenite in the same grain, possibly indicating exsolution of sphene.

Large calcite porphyroblasts are common in some chlorite-amphibole schists. Textural studies show that they have generally grown along foliation planes and fractures and often enclose remnants of the pre-existing (s_2 and s_3) foliations indicating that they were formed post-tectonically, possibly by the late introduction of carbonate-rich fluids.

A horizon of actinolite-schist mapped west of Elisenheim consists entirely of radiating needles of actinolite, up to 5 cm long with the exception of scattered grains of quartz (see Plate 17).

4.2.2. Porphyroblastic Amphibolite

The characteristic feature of this type of amphibolite is the presence of large xenoblastic amphibole porphyroblasts (up to 5 mm across) set in a fine- to medium-grained mosaic of generally untwinned plagioclase,

Plate 17. Radiating actinolite needles. Crossed nicols, SF11, Actinolite schist.

chlorite, epidote, biotite, minor quartz, K-feldspar and opaques (Plate 19). The estimated modal composition of a typical example of this amphibolite is given in Table 7.

The mineral assemblages typical of porphyroblastic amphibolites are:

(a) Hornblende-actinolite-plagioclase-epidote-chlorite-K-feldspar-garnet-rutile

(b) Hornblende-actinolite-plagioclase-epidote-chlorite-K-feldspar-calcite-garnet

The amphibole porphyroblasts comprise roughly equal amounts of hornblende and actinolite which coexist either as patches within grains (Plate 18) or with hornblende forming rims around actinolite cores (Plate 20). Discrete actinolite and hornblende grains were not recognised in any of the amphibolites. The colour of hornblende parallel to the γ-axial colour is blue green. This colour is the same throughout the Elisenheim area but may change over a larger area with increasing grade to green, brown-green, brown due to increasing Ti relative to Fe (Binns, 1965).

The co-existing amphiboles were distinguished primarily on the basis of colour and pleochroism. The hornblende is pleochroic deep green to blue green and co-existing actinolite is nearly colourless, slight pleochroic from pale blue-green to green. A difference in birefringence accompanies the colour difference with actinolite having the higher order interference colours. The actinolite cores and patches have larger optic axial angles and lower refractive indices than the hornblende peripheries (Table 5). Contacts between the co-existing amphiboles are irregular in shape but are sharp and display a Becke line

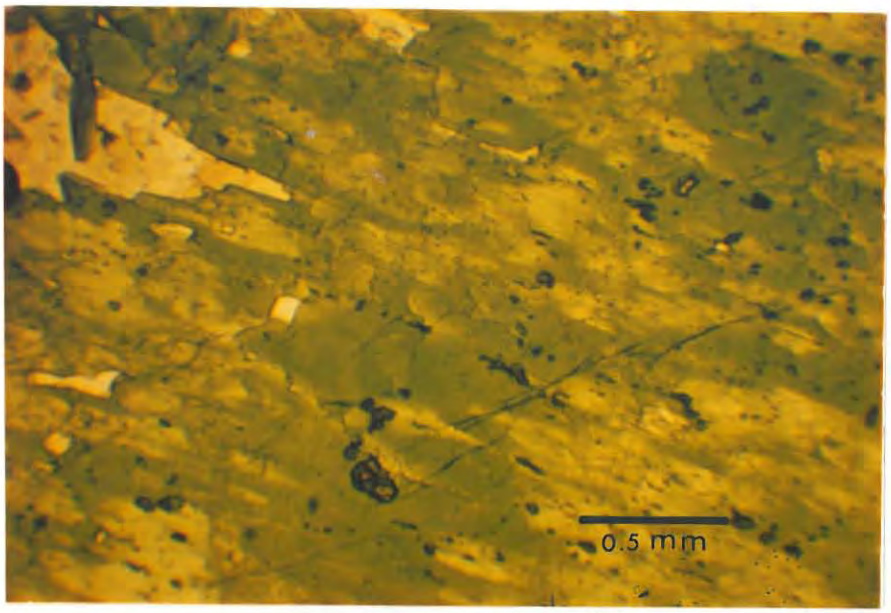

Plate 18 Patchy hornblende-actinolite intergrowths in Matchless amphibolite. Plane polarisedllight. Hornblende dark green, actinolite yellow.

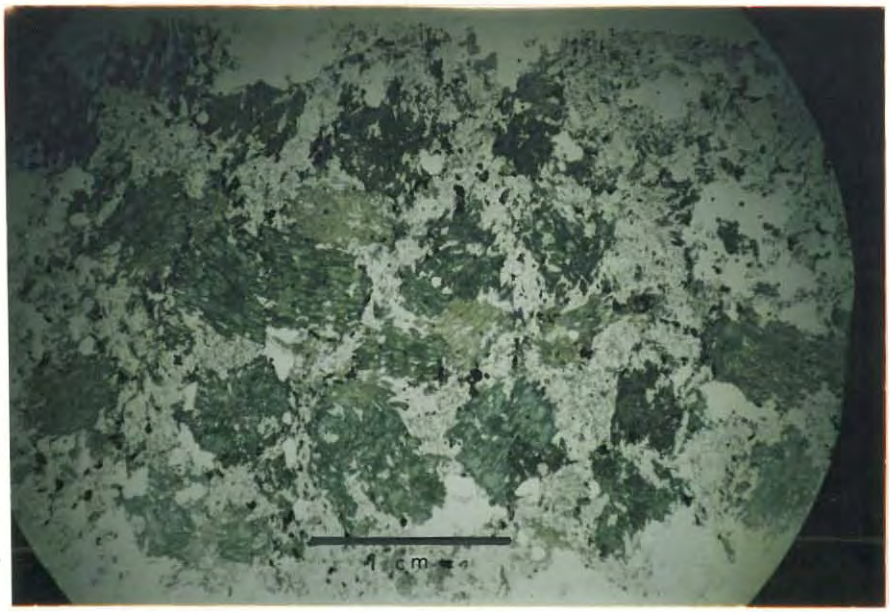

Plate 19. Patchy hornblende-actinolite intergrowths in amphibole porphyroblasts. SF93, porphyroblastic amphibolite. Plain light.

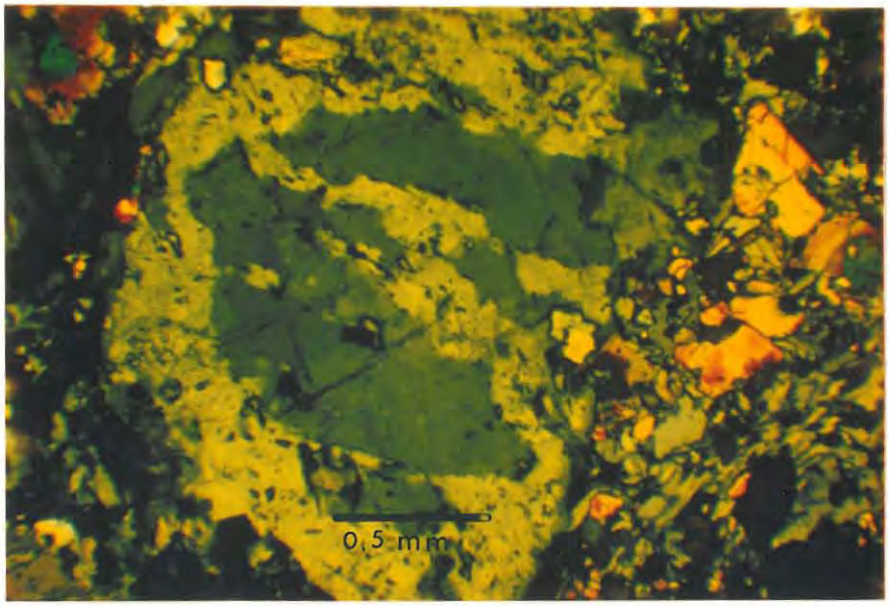

Plate 20. Hornblende core enclosed by actinolite and rimmed by hornblende in zonal arrangement. Matchless amphibolite. Plane polarised light.

when orientated almost parallel to the axis of the microscope.

Zoned plagioclase grains were rare. Composition of grains ranged between An_{25} and An_{40}. Aggregates of chlorite are clustered around the amphibole porphyroblasts and coexist with biotite and minor amounts of muscovite. Large biotite grains have occasionally grown in the centre of the amphibole grains. Minor amounts of sphene and ore are scattered throughout samples along with aggregates of granular epidote.

Table 6. Refractive index and optic axial angle determinations on co-existing actinolite and hornblende.

	Actinolite	Hornblende
α	1.644	1.655
β	1.652	1.670
γ	1.662	1.676
2V	$\sim 80^{\circ}$	$\sim 60^{\circ}$

4.2.3. Epidote amphibolite

This group is generally finer grained than the porphyroblastic amphibolites and contains large amounts of epidote (see Table 7). The typical mineral assemblage is:-

(a) Hornblende-actinolite-epidote-plagioclase-calcite-magnetite

Xenoblastic amphibole porphyroblastesis is common with all grains (maximum diameter of 2 mm) showing actinolite-hornblende zoning. The zoning is not as strongly developed as in the porphyroblastic amphibolites and hornblende is the dominant phase. Plagioclase is less abundant than in the other varieties of amphibolite and forms a fine-grained mosaic (0.1 mm to 0.5 mm) of generally unzoned and untwinned grains. Plagioclase composition determinations on the occasional twinned grains indicates that the plagioclases are surprisingly sodic with a content falling between An_{25} and An_{40}. This composition is similar to that of the porphyroblastic amphibolites despite the fact that whole rock chemical analyses indicate that the epidote amphibolites are highly calcic. The plagioclase grains, as in the other amphibolites, are fresh and unsaussuritised.

Granoblastic epidote and plagioclase grains form a matrix interstitial to the amphibole porphyroblasts. The epidote is yellowish-green and slightly pleochroic and biaxial negative with a large 2V. Birefringence is strong. Elongate sections are commonly rare but extinction was found to be inclined to a number of grain boundaries. Calcite is abundant

Table 7. Estimated modal compositions in volumetric percentage of three Matchless amphibolites.

Mineral	Chlorite amphibole schist, SF77	Porphyroblastic amphibolite, SF74	Epidote amphibolite, SF69
Hornblende Actinolite	36	41	46
Plagioclase	28	21	11
Epidote	3	18	33
Chlorite	25	12	1
Biotite	2	2	1
K-feldspar	-	3	-
Quartz	2	-	-
Sphene	1	-	-
Calcite	2	-	6
Garnet	-	tr	-
Ore	1	2	2

and comprises up to 10% of some specimens. The grains are 1 mm to 2 mm across and appear both as incipient porphyroblasts poikiloblastically enclosing hornblende and epidote and as grains that have grown later along foliation planes. The latter development possibly indicates late- or post-tectonic introduction of carbonate-rich fluids. Minor amounts of biotite, chlorite and opaques are scattered throughout the rock.

The epidote amphibolite is generally massive and unfoliated and forms the "cores" of the boudins previously interpreted (Viljoen in Anhausser and Button, 1974) as being pillow structures. These boudins are comprised of massive epidote amphibolite surrounded by highly sheared "selvedges" of quartz hornblende schist. The schist consists of approximately 60% lath-like hornblende and 30% granoblastic quartz with minor amounts of granoblastic epidote, flakes of chlorite, opaque ore and apatite. Massive sugary quartz is usually concentrated in the "tail-edges" of the boudins. These mineralogical differences between "selvedges" and "core" are in agreement with the findings of Kröner (1974) who studied boudins at Matchless Mine. (The chemical composition of a "core" (sample SF69) is presented in Tables 8 and 10).

4.2.4. Discussion

The mineral assemblages of the amphibolites are typical of the amphibolite facies (Turner, 1968). The first appearance of almandine-garnet in regionally metamorphosed rocks is not yet known but conditions of at least 4 kb at 500°C must be exceeded to stabilize this phase (Winkler, 1974). According to Winkler (1974) the first appearance of almandine coincides with the first appearance of hornblende (instead of actinolite) in mafic schists. This reaction invariably takes place in the higher range of low grade metamorphism. If an iron-poor, colourless or pale-green actinolite is present in a mafic schist the formation of green hornblende takes place according to (curve 8 in Fig. 6):

(8) actinolite + clinozoisite + chlorite + quartz = hornblende

Due to the complex compositions of the minerals taking part in the reaction, a certain range of P, T conditions allows actinolite to persist with hornblende until a somewhat higher temperature has been attained. The positioning of curve (8) in Figure 6 is a further indicator of the P, T conditions operative during metamorphism of the Elisenheim rocks. It is probable that reaction (8) will have some bearing on the origin of the zoned actinolite/hornblende grains. The decrease or disappearance of hornblende and biotite in mafic rocks can take place by a number of reactions (De Waard in Winkler, 1974):

(9) hornblende + quartz = hypersthene + clinopyroxene + plagioclase + H_2O

(10) hornblende + biotite + quartz = hypersthene + k-feldspar + plagioclase + H_2O

(11) hornblende + almandine + quartz = hypersthene + plagioclase + H_2O

No pyroxenes are present in the Matchless amphibolites and the P, T conditions necessary for these reactions have not been attained.

The coexistence of hornblende and actinolite is common in upper greenschist facies and lower amphibolite facies rocks. Occurrences

have been reported by Shido (1958), Klein (1968, 1969), Cooper and Lovering (1970), Choudhuri (1972, 1974), Brady (1974), Graham (1974) and Grapes (1975). The presence of an optically and chemically sharp interface between the coexisting calciferous amphiboles has prompted several writers (Shido, 1958; Klein, 1969; Cooper and Lovering, 1970 and Brady, 1974) to propose the existence of a miscibility gap in the calciferous amphibole series between hornblende and actinolite which according to Ernst (1968), is due to the existence of a solvus within the Ca group of amphiboles.

Shido (1958) states that the refractive indices of coexisting actinolite and hornblende are related and that this supports the presence of a miscibility gap between these two groups of amphiboles under the metamorphic conditions prevailing in zones A and B of the Nakoso and Iritono districts of the Central Abukuma Plateau. He does not preclude the possibility that the miscibility gap may vanish in other types of metamorphism and also states that the zonal structure of the amphiboles might be due to insufficient diffusion during metamorphic recrystallisation and not due to the existence of a miscibility gap. He discounts the latter possibility by showing that the hornblende and actinolite groups occupy chemically separate composition fields.

In a study of two-amphibole assemblages Klein (1969) found optically- and chemically-sharp contacts between the amphiboles and suggests that the highly complex and patchy intergrowths in single grains (similar to Plate 18) do not provide clear evidence for replacement of one amphibole by another. Furthermore he believes that the sharp interface excludes the possibility of a complete compositional range between the two groups, which, can rather be considered as an equilibrium pair which have crystallised simultaneously as points across a miscibility gap. Similar conclusions have been reported by Cooper and Lovering (1970) from the Haast Schists of New Zealand and by Brady (1974) from garnet zone and staurolite-kyanite zone amphibolites of the Ammonoosuc Volcanics of New Hampshire.

Graham (1974) is of the opinion that textural and chemical evidence does not indicate the presence of any miscibility gap between hornblende and actinolite in the metabasites within the chlorite to garnet zones of the southwest Scottish Highlands. He states that while petrographically distinct actinolite and blue-green hornblende may occur together at all grades of metamorphism in the southwest Highlands, they are often, but not invariably, separated by a sharp Becke line. Besides, petrographically (and chemically) intermediate amphibole types are observed more and more commonly from the lower chlorite to garnet zones. He believes that these petrographic features commonly observed in hornblende-actinolite pairs in the Scottish Dalradian, and perhaps also in metabasites of other metamorphic terrains, may be indicative of the non-attainment of chemical equilibrium consequent upon the sluggish and incomplete equilibration of low-grade actinolites during prograde metamorphism.

This conclusion is supported by Grapes (1975) who states that although chemical data indicate a chemical discontinuity between coexisting actinolite and hornblende, textural evidence strongly suggests replacement of "relic" actinolite and that the amphibole pairs do not represent an equilibrium pair.

Graham (1974) interprets the general tendency of hornblende rims and overgrowths, to enclose actinolite cores and patches, as a reaction texture

in which actinolite cores represent relics of an earlier lower-grade (actinolitic greenschist) stage of prograde metamorphism and the hornblende rims the result of reaction between actinolite and adjacent phases. Reference to Plate 20, which depicts a common feature in Matchless amphiboles, raises some doubt as to the feasibility of this mechanism, as the central hornblende (when considered in two dimensions) could not have been in contact, in the form of actinolite, with any non-amphibole phases with which to equilibrate itself during prograde metamorphism.

The present writer does not dispute the existence of a chemical discontinuity between the two coexisting amphibole groups but believes that, despite the highly complex and patchy nature of the intergrowths, that the actinolite formed before hornblende (and not simultaneously) and that it has not been entirely consumed in the formation of the latter during prograde metamorphism. It is probable that shearing deformation (prevalent during the B_2 phase) has caused an overstepping of the physical and chemical conditions of metamorphism so that complete compositional readjustment of the amphiboles was not achieved (Grapes, 1975, p. 137). The conclusion that the coexisting amphibole pairs have formed due to non-equilibration during prograde metamorphism is strengthened by the fact that Choudhuri (1974) has demonstrated, from a study of Mg, Fe and Al distributions that actinolite was active in hornblende-forming reactions in upper greenschist metagraywackes. Furthermore Rimsaite (1974) has shown that retrograde metamorphism in the Archean greenstone belt in the Malartic area, Quebec, has produced a zonal sequence (retrograde actinolite and tremolite rimming prograde hornblende) opposite to that observed in prograde terrains.

Chlorite coexists with epidote, hornblende, quartz and plagioclase and appears to have formed during prograde metamorphism. The abundance of chlorite in the chlorite-amphibole schists is probably a function of the high magnesian content of the schists.

Plagioclase is mainly oligoclase to andesine (An_{25-40}) and is characteristic of the change from low to medium grade metamorphism (greenschist facies to amphibolite facies) which is represented by curve (9) in Figure 6. Zoned and occasionally twinned plagioclases are not uncommon in the chlorite amphibole schists but are rare in the amphibolites. The zonal structures are indistinct but appear to be two-layered. The inner zone is always more sodic (An_{0-10}) than the outer zone (An_{25-40}) indicating that the zoning was produced during prograde metamorphism.

Metamorphism has outlasted F_3 deformation and is evidenced by garnet, biotite, and hornblende grains randomly orientated across the foliation.

Chemical analysis of the amphibolites has shown that the epidote amphibolites contain anomalously high calcium values and that their present composition departs from the expected trend of differentiation of the amphibolites. This difference may be accounted for by Ca-metasomatism (see Chapter 5).

A number of samples of epidote amphibolite, porphyroblastic amphibolite and chlorite-amphibole schist were found to contain veins of calcite cutting obliquely across the foliation and post-tectonic porphyroblasts of calcite scattered randomly throughout. Most of the porphyroblasts contain remnants of the pre-existing foliation and definitely appear to have

grown after the development of the surrounding material.

The writer believes that the above petrographic evidence suggests calcium-rich and CO_2 fluids metasomatised the amphibolites after the F_3 tectonism and that this metasomatism affected all the amphibolite horizons to a greater or less degree. The fact that only the epidote amphibolites contain high Ca and CO_2 values could be due to preferential sampling of poorly metasomatised chlorite-amphibole schists and porphyroblastic amphibolites and highly carbonated epidote amphibolites.

4.3. Ultrabasic Association

4.3.1. Talc Schists

The talc schists of northwest Elisenheim are similar mineralogically to those recorded from Otjihase Mine (Vellet, personal communication) and can be shown to be chemically related to the basic units of the amphibolite belt (see Chapter 5). They are therefore considered to be part of the Matchless meta-igneous suite that were intruded or extruded at a different stratigraphic level from the rest of the Matchless amphibolite rocks.

Most of the talc body is comprised of folded and crenulated, pale-green, dolomitic talc-schist with varying amounts of chlorite, magnetite and quartz. The schists are poorly mineralised by countless specks of malachite and disseminations of oxidised sulphides.

Under the microscope the talc schists consist of well-foliated plates of talc, chlorite and minor amounts of actinolite in parallel alignment. Magnetite grains have grown within the foliation. Bands of tiny interlocking quartz grains are parallel to the foliation. The amounts of talc, chlorite, amphibole and quartz are variable with the schists grading from pure talc schists into chlorite amphibole schists. The most striking feature of the rocks is the post-tectonic growth of abundant rhombohedral carbonate porphyroblasts across the foliation. The porphyroblasts are restricted to the most talcose schists and were identified by X-ray diffraction techniques as dolomite containing minor calcite. The dolomite rhombs range in size from 1 mm to 20 mm and weather to brown vugs.

Narrow bands and lenses of dolomitic-chlorite schist, talc-chlorite schist, chlorite schist, actinolite-talc schist and quartz-talc-magnetite schist are intercalated within the dolomitic talc schists. Small lenses of brown marble were infrequently mapped with the ultramafic body.

4.3.2. Discussion

Geochemical analysis of three talc schists proves that the rocks are ultramafics and do not represent a suite of metamorphosed impure siliceous dolomites. Mineral textures indicate that the processes that formed the talc were operative before F_2 deformation. The dolomite rhombs are relatively undeformed and grew after F_3 tectonism.

Viljoen and Viljoen (1969, p. 42) state that although serpentinisation is the main process which drastically affects the original chemistry and mineralogy of peridotitic rocks in the Barberton region, steatization and

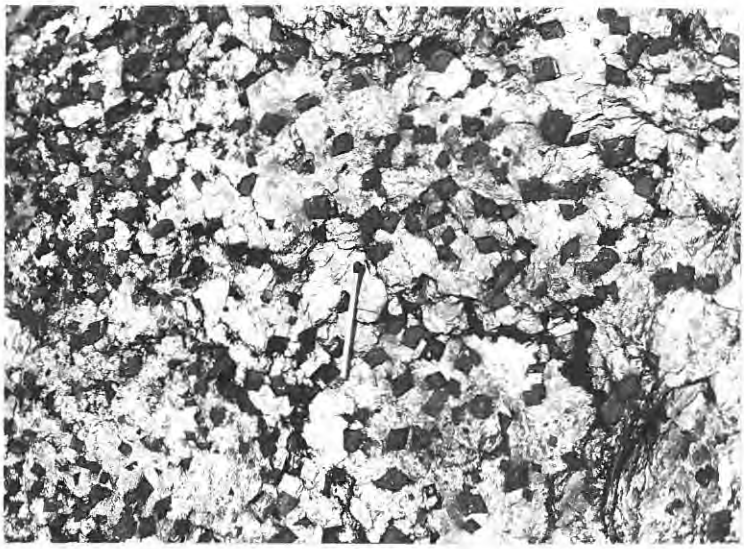

Plate 21. Dolomite porphyroblasts in talc schist.

probable CO_2 metasomatism also appear to have been effective. Steatization of ultrabasic rocks, defined by Hess (1933) as

> " ..... that process of hydrothermal alteration of an ultrabasic which in its final stages results in the formation of a talcose rock",

may be accomplished simply by addition of silica, and in some cases water, to serpentinised peridotites. More commonly CO_2 metasomatism is involved and dolomite or magnesite then appear as constituent phases of the end product. Steatization often follows serpentinisation and is a hydrothermal process connected with the intrusion of a granite magma. Hess (1933), however, states that there are often cases where the only available solutions are the ultrabasic body itself or the enclosing geosynclinal sediments and that steatization is then the local aftermath of serpentinisationccaused by prolonged activity, at lower temperatures, of waters similar in origin to those which had been responsible for earlier serpentinisation.

The mineral series hornblende, actinolite, chlorite, talc and carbonate is characteristic of steatization (Hess, 1933). This process is retrograde and alteration takes place with continuously decreasing temperature. If the temperature of formation is high then hornblende will be the first mineral to form otherwise any lower temperature mineral may form. Similarly, alteration may stop with any member of the series, provided the solutions are removed from contact with the ultrabasic body before the temperature has fallen sufficiently low for talc and carbonate to form.

Talc may form during steatization of an ultrabasic body by either of the two reactions (Hess, 1933):

(12) by simple addition of CO_2,

serpentine + CO_2 = talc + magnesite + H_2O

(13) if solutions are lime bearing,

serpentine + CaO + CO_2 = talc + dolomite + MgO + H_2O.

It is probable that the solutions present at the time of intrusion of the ultramafics were not enriched in lime and that reaction (12) took place. This is suggested by the absence of pre-tectonic lime-metasomatism of the amphibolites.

According to Turner and Verhoogen (1960, p. 580), talc becomes unstable when exposed to solutions rich in CaO at low metamorphic temperatures and sufficiently high pressures of CO_2 and undergoes progressive replacement by dolomite through the following reaction:

(14) Talc + CaO + CO_2 = Dolomite + MgO + SiO_2 + H_2O
(removed in solution)

It is suggested that this reaction is indicative of the conditions prevailing after F_3-deformation which gave rise to the growth of the idioblastic rhombohedral dolomite porphyroblasts. Solutions of similar composition (rich in CO_2 and lime) are thought to have metasomatised the Matchless amphibolites to varying degrees after F_3 deformation. It is possible that the solutions that altered the two horizons are one and the same.

5. GEOCHEMISTRY

5.1. Introduction

The objectives of this study have been primarily to ascertain whether the basic and ultrabasic rocks of the Matchless Amphibolite belt of the Windhoek district are igneous in origin, and if so, to determine the chemical variations between the various units and to compare the chemistry of these rocks with well-established classes of igneous rocks.

Chemical analyses were determined on twenty samples from the Elisenheim and Matchless Mine areas. These include two pelitic schists, seven porphyroblastic amphibolites, four epidote amphibolites, and four chlorite-amphibole schists. Three talc schists from an ultramafic body outcropping within Khomas schists seven kilometres north of the Matchless Amphibolite belt on Elisenheim were also analysed.

Major element oxides and the trace elements Ba, Nb, Zr, Y, Rb and Sr were determined by X-ray fluorescence analysis and Co, Ni and Cr_2O_3 values were determined by Atomic Absorption spectroscopy. FeO contents were determined volumetrically and H_2O^-, H_2O^+ and CO_2 gravimetrically. All analyses were undertaken by the General Superintendence Company on behalf of the National Institute for Metallurgy, Johannesburg. Duplicate determinations for the trace elements Nb, Zr, Y, Sr and Rb were made on samples SF49, SF59, SF84, SF73, SF83, SF16, SF81, SF1, SF80 by the writer. Analyses were undertaken on pressed powder discs against standard samples GSP-1, BCR and OK-272, using a Phillips PW 1540 manual spectrometer and PW 1130/90 generator. It was found that there was generally good agreement between N.I.M's results and those obtained by the author.

5.2. Basic and Ultrabasic Associations

This discussion is restricted to the basic and ultrabasic rocks that comprise the Matchless Amphibolite belt and account for the majority of the basic rocks of the area. The occasional, narrow bands and lenses, less than 10 cm wide, of amphibolitic material which lie within Khomas schists and which possibly formed by metasomatism of sedimentary layers (Orville, 1969, p. 64) are not discussed in any detail. The basic and ultrabasic units are discussed together in one section, since their chemistry and origins are possibly intimately related.

The effects of metamorphism on the chemistry of the Matchless amphibolites is discussed as an introduction.

Various writers (Leake, 1964; Orville, 1969; Kalsbeek & Leake, 1970; Preto, 1970) in their treatments of the "amphibolite problem", have assumed that during metamorphism individual rock layers acted essentially as closed systems and that metasomatism did not occur to a significant degree. For example, Kalsbeek and Leake (1970) have proved that, despite large scale migmatisation and veining, the chemical composition of certain Greenland amphibolites has hardly changed from that of the parent basic igneous material. Engel and Engel (1962), however,

demonstrated in their account of progressive metamorphism of amphibolite in the Adirondacks that certain chemical differences took place between amphibolites in the amphibolite facies and those in granulite facies terrains. They concluded that these differences were the results of metamorphism and found that with increasing temperature there was a decrease in H_2O, K_2O and Fe_2O_3 and an increase in Ca and Mg. These chemical migrations have been largely confirmed by Elliott (1973) during a study of gabbro/amphibolite pairs. Elliott (1973) emphasises that the observed movements apply only to the transition of amphibolite from higher facies and should not be extrapolated to the entire range of matamorphic facies. Similarly, Field and Elliott (1974) have shown that metamorphism of hyperite to amphibolite is not isochemical and that trace elements Rb and possibly Zr were increased and Zn diminished.

Miyashiro (1975) states that the plot Na_2O/K_2O versus $Na_2O + K_2O$ helps to clarify the nature and extent of migration of Na_2O and K_2O, which, along with CaO and H_2O, are particularly migrant in greenschist facies metamorphic rocks but less so under conditions of amphibolite facies metamorphism . Miyashiro (1975) has plotted the compositions of a great number of fresh Quaternary volcanic rocks and states that rocks plotting above curve V-V (see Figure 7) owe their compositions to post-igneous changes. The Matchless basic and ultrabasic rocks plot below this curve which suggests that they have not undergone post-igneous changes, however, this does still not preclude the possibility limited alkali migration.

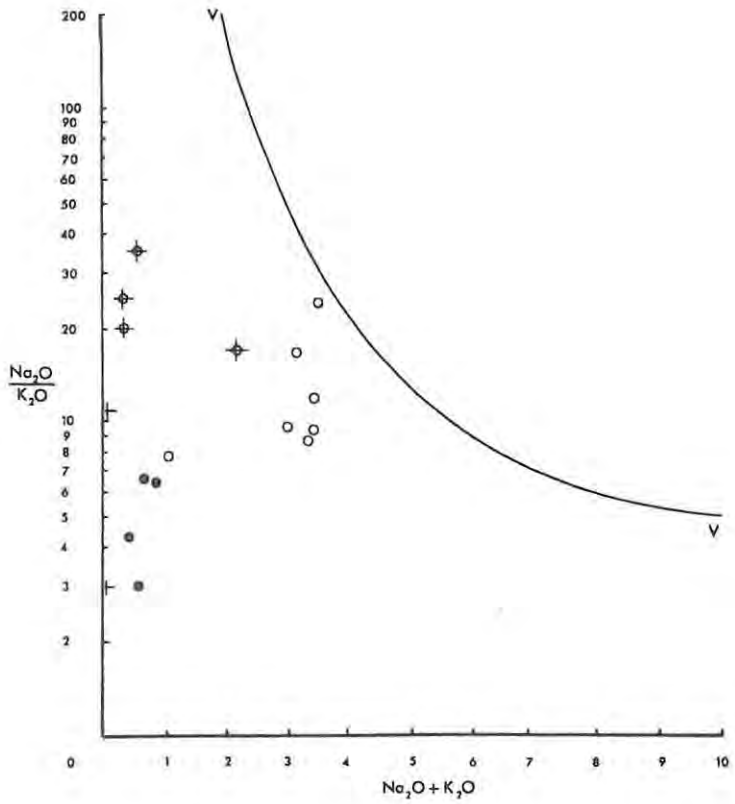

Figure 7 . Na_2O/K_2O versus $Na_2O + K_2O$ diagram of Matchless rocks (after Miyashiro, 1975). See Figure 8 for symbols.

Mehnert (1969) believes that under normal conditions of regional metamorphism the bulk composition of whole rocks remain generally unchanged and that chemical migrations are restricted to relatively small domains. In light of the aforegoing discussion it is assumed that the Matchless amphibolites behaved essentially as closed systems and that metamorphism has not camouflaged the obvious chemical similarities between the parent basic igneous material and the present metamorphosed equivalents. That is, except for the steatization of the ultramafics and the post-tectonic Ca-metasomatism and/or calcite veining of the talc schists and some amphibolites.

5.2.1. Major Elements

The petrographic recognition of three different types of amphibolite (epidote amphibolite, porphyroblastic amphibolite and chlorite-amphibole schist) and one talc schist with ultrabasic affinities has been substantiated by obvious petrochemical characteristics. Reference to Table 8 indicates that in the series, epidote amphibolite through porphyroblastic amphibolite to chlorite-amphibole schist, FeO, total Fe and MgO systematically increase while there is a corresponding reduction in Fe_2O_3. SiO_2 values are erratic and range between 41% and 49%. K_2O is low (average 0.14%) in all the amphibolites and the epidote-amphibolites are enriched in CaO and CO_2. The talc schists have high MgO values (average 23.57%) and low Al_2O_3 (average 0.85%).

Lithotype	Epidote Amphibolite				Porphyroblastic Amphibolite						Chlorite-amphibole Schist				Talc Schist		
Sample No.	SF43	SF59	SF69	SF84	SF73	SF74	SF75	SF77	SF82	SF83	SF85	SF14	SF16	SF76	SF91	SF1	SF3	SF80
SiO_2	45,82	42,79	43,79	47,47	49,85	48,82	43,59	49,88	49,14	47,18	49,51	41,46	47,43	41,36	45,82	49,69	57,21	59,41
TiO_2	1,62	1,79	1,76	1,75	1,83	1,64	1,82	1,73	2,24	1,78	1,58	1,18	0,65	1,39	2.51	0,01	0,01	0,02
Al_2O_3	14,03	13,62	14,26	12,75	16,08	15,66	11,90	13,93	14,77	14,96	15,49	10,17	6,97	8,60	14,29	1,24	0,71	0,62
Fe_2O_3	5,44	5,81	6,20	5,08	3,23	2,60	3,69	3,08	2,81	2,15	3,01	2,00	2,26	2,58	3,44	0,47	0,12	0,13
FeO	5,17	5,15	4,99	4,62	6,86	6,73	10,32	7,95	8,81	8,09	7,28	10,76	9,64	12,45	10,47	3,90	4,37	4,30
MnO	0,20	0,22	0,20	0,22	0,19	0,15	0,27	0,24	0,21	0,18	0,21	0,26	0,28	0,31	0,27	0,17	0,10	0,04
MgO	4,62	4,76	3,97	4,08	6,42	8,57	14,19	7,72	8,18	8,13	8,18	20,03	18,11	16,93	9,87	17,35	24,84	28,52
CaO	17,08	15,23	18,15	17,63	9,22	9,82	8,58	9,38	7,19	8,24	9,14	7,20	9,49	8,50	6,82	10,66	2,98	0,38
Na_2O	0,71	0,34	0,53	0,39	3,01	2,67	0,92	3,12	3,34	2,98	3,02	0,20	0,35	0,25	2,08	0,15	0,03	0,11
K_2O	0,11	0,08	0,08	0,13	0,34	0,28	0,12	0,26	0,14	0,18	0,34	0,01	0,01	0,01	0,12	0,30	0,01	0,01
P_2O_5	0,62	0,40	0,53	0,46	0,25	0,25	0,23	0,24	0,35	0,24	0,23	0,21	0,22	0,22	0,33	0,24	0,04	0,01
CO_2	2,94	1,01	4,34	3,98	1,02	0,69	0,98	0,62	0,44	3,22	0,05	0,06	0,12	2,21	0,05	12,61	4,55	0,54
H_2O^-	0,04	0,08	0,15	0,08	0,13	0,11	0,14	0,24	0,10	0,11	0,10	0,04	0,02	0,47	0,13	0,11	0,13	0,12
H_2O^+	1,59	1,74	0,86	1,28	0,93	1,46	3,25	1,03	1,99	1,91	1,69	6,10	4,05	4,34	3,39	2,23	3,91	4,84
Total	99,99	100,02	99,81	99,92	99,36	99,45	100,00	99,43	99,71	99,35	99,83	99,68	99,60	99,62	99,59	99,13	99,01	99,05
FeO*/MgO	2,18	2,18	2,66	2,25	1,52	1,06	0,96	1,39	1,39	1,23	1,22	0,63	0,64	0,87	1,37	0,25	0,18	0,15
Discriminant Function																		
X_3	2,212	1,367	1,811	1,536	1,404	1,771	4,173	2,366	3,385	2,496	1,509	3,480	1,703	4,771	4,350	n.d.	n.d.	n.d.

Analyst: General Superintendence Co., Johannesburg.

FeO* = Total iron as FeO.

Table 8. Major element chemical analyses of 15 Matchless amphibolites and 3 talc schists.

The problem of distinguishing between amphibolites that result from the metamorphism of basic igneous rocks and those formed during the metamorphism of sedimentary horizons has concerned geologists for many years. Various writers (Leake, 1964; Orville, 1969; Kalsbeek and Leake, 1970) have shown that the most definite distinction between ortho- and para-amphibolites lies in comparing the trends of variation of certain critical elements rather than by comparing the differences in the absolute values of the chemical components. Where multiple analyses are available, this seems a most fruitful line of approach, because amphibolites which have the composition of igneous rocks and, in addition, show an igneous trend of chemical variation instead of an opposed sedimentary trend are almost certainly of igneous origin.

Following the methods outlined by Leake (1964) the analyses of eighteen basic and ultrabasic rocks were recalculated to Niggli values. These values are presented in Table 9. Niggli values mg and c are plotted in Figure 8, which illustrates the trend line of a typical differentiated basic igneous series, in this case the Karoo dolerites, as well as the fields of typical pelites and dolomites and the trend lines of sedimentary mixtures. It is clear that the analysed amphibolites and talc schists, with the exception of the epidote-amphibolite variety, follow roughly the trend of the Karoo dolerites. The departure from this trend line by the epidote amphibolites could be due to calcium-enrichment during metamorphism since the trends evident in Figures 9, 11, 13 and 14 indicate that the epidote amphibolites are possibly the most highly differentiated units in a basic igneous series and that the only departure from this series is due to an increase in calcium.

The points plotted in Figure 9 again follow a trend roughly parallel to that of basic igneous rocks and opposed to the trends expected for various sedimentary mixtures. The fields occupied by typical pelitic and carbonate sediments and basic igneous rocks in comparison with the Matchless amphibolites are illustrated by means of an ACF diagram in Figure 10. Reference to this plot shows that the mean value of the porphyroblastic amphibolites and the mean of all three types of amphibolite plot adjacent to Poldervaart's (1955) average amphibolite within the field of basic igneous rocks. The average of the epidote amphibolites plots within the field of shale-carbonate sedimentary mixtures and the chlorite-amphibole schists towards the "F" corner of the diagram within the field of ultrabasic rocks (Winkler, 1967). Orville (1969, p. 73) believes that amphibolites falling within the field of basic igneous rocks are igneous in origin, since most carbonate and shale mixtures as they occur in common sediments, do not fall within the basalt field. Consequently, it appears that, despite the apparent sedimentary composition of the epidote amphibolites, that the Matchless amphibolites are igneous in origin.

Numerous authors have, in the aforegoing discussion, attempted to use one, two, or at the most three elements at once as a means of distinguishing ortho- and para-amphibolites. Shaw and Kudo (1965), on consideration of the methods of multivariate statistical analysis, have applied the discriminant function test to the amphibolite problem. Discriminant functions X_1 and X_2 were calculated for trace elements and X_3 for major elements. The Matchless amphibolite samples were not analysed for Sc and V which does not permit the calculation of functions X_1 and X_2. The discriminant function, $X_3 = 7.07 \log TiO_2 + 1.91 \log Al_2O_3 - 3.29 \log Fe_2O_3 + 8.48 \log FeO + 2.97 \log MnO + 4.81 \log MgO + 7.80 \log CaO + 3.92 \log P_2O_5 + 0.15 \log CO_2 - 15.08$ when calculated will

Table 9. Niggli values of 15 amphibolites and 3 talc schists.

Sample No.	c	mg	fm	al	alk
SF49	42,92	0,44	35,90	19,39	1,79
SF59	40,29	0,44	38,95	19,82	0,93
SF69	45,05	0,39	34,19	19,47	1,29
SF84	46,49	0,43	33,88	18,50	1,14
SF73	24,55	0,53	44,08	23,56	7,80
SF74	24,73	0,62	47,36	21,47	6,44
SF75	18,49	0,64	65,47	14,10	1,94
SF77	23,97	0,55	48,84	19,57	7,61
SF82	18,60	0,55	52,34	21,02	8,04
SF83	21,45	0,58	49,81	21,43	7,30
SF85	22,98	0,58	48,21	21,42	7,37
SF14	14,22	0,73	74,37	11,05	0,36
SF16	19,63	0,72	71,78	7,93	0,66
SF76	17,51	0,66	72,62	9,75	0,47
SF81	17,12	0,53	58,22	19,74	4,91
SF1	27,23	0,87	70,22	1,75	0,80
SF3	7,18	0,90	91,79	0,95	0,08
SF80	0,87	0,91	98,11	0,78	0,24

be positive for an ortho-amphibolite and negative for a para-amphibolite. Shaw and Kudo (1965) state that the probability of incorrect classification is 5.7% and that the most important oxides for discrimination are TiO_2, FeO and P_2O_5. Calculation of X_3 for the Matchless amphibolites has yielded positive values (Table 8) for all the amphibolites which according to Shaw and Dudo (1965) is characteristic of ortho-amphibolites.

The systematic variation in FeO*/MgO ratios (Table 8) is suggestive of control by igneous differentiation. Miyashiro (1975) states that low FeO*/MgO values are observed in highly cumulative rocks while some late differentiates with $SiO_2 \sim 54\%$ show FeO*/MgO up to 2,8.

It is apparent from the major element chemical data that the units of the Matchless amphibolite studied in the Windhoek area are igneous in origin and were possibly derived from an igneous differentiation series.

5.2.2. Trace Elements

Leake (1964) and Kalsbeek and Leake (1970) have shown that Cr and

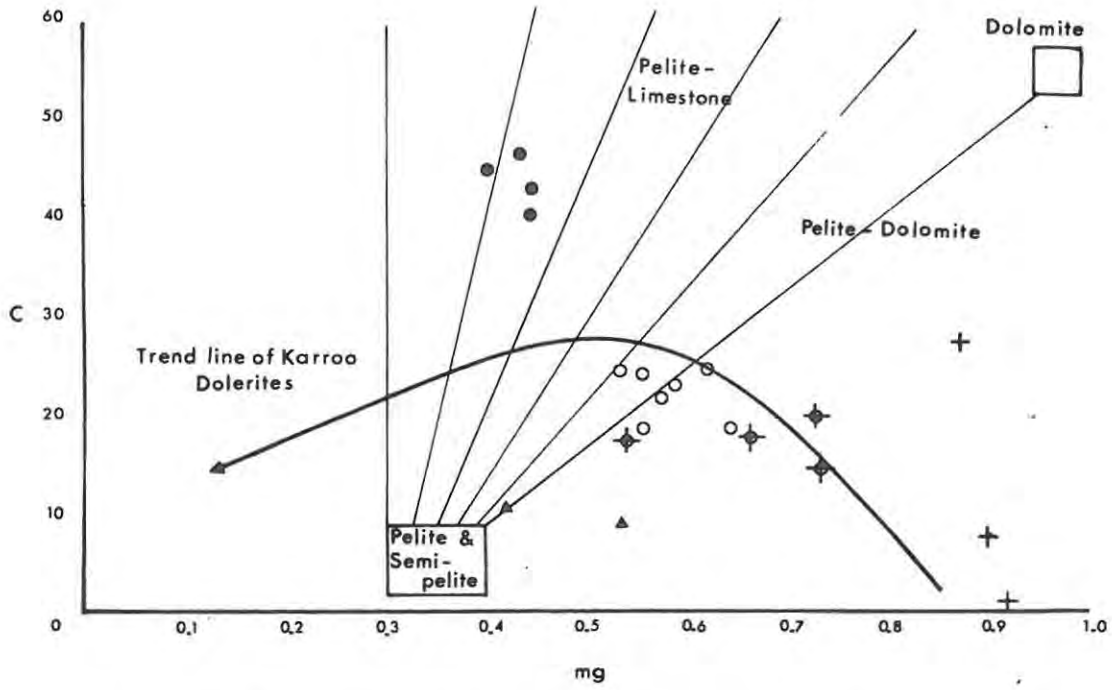

Figure 8. Plot of Niggli mg vs c (after Leake, 1964). Symbols:- ▲ Khomas schist; ● epidote amphibolite; ○ porphyroblastic amphibolite; ⊕ chlorite amphibole schist; + talc schist.

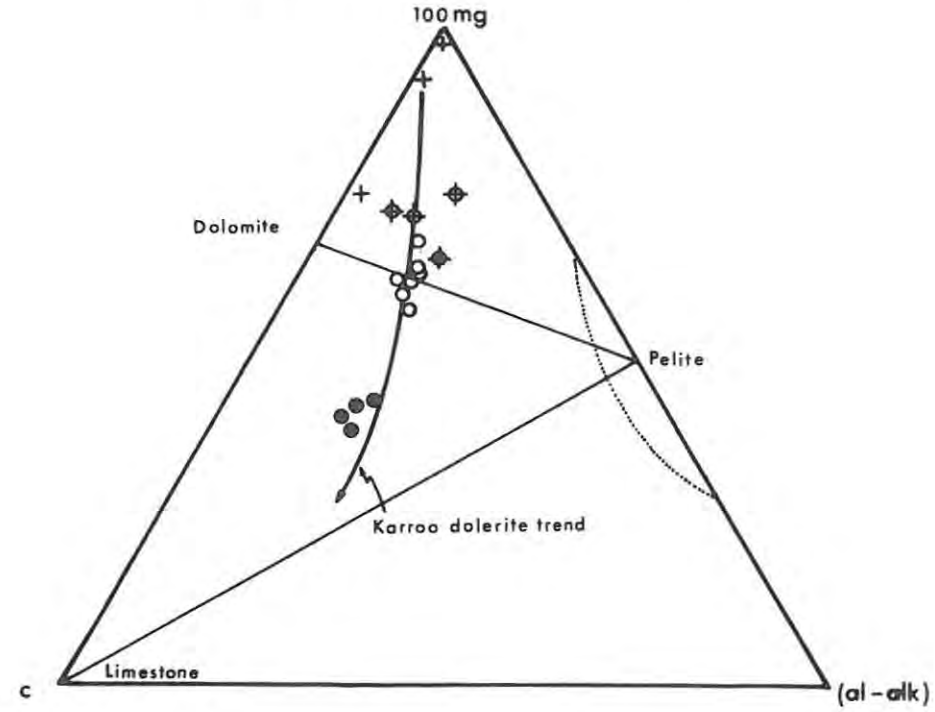

Figure 9. Plot of Niggli 100mg - c - (al-alk). Symbols as in Figure 8 (after Kalsbeek and Leake, 1970).

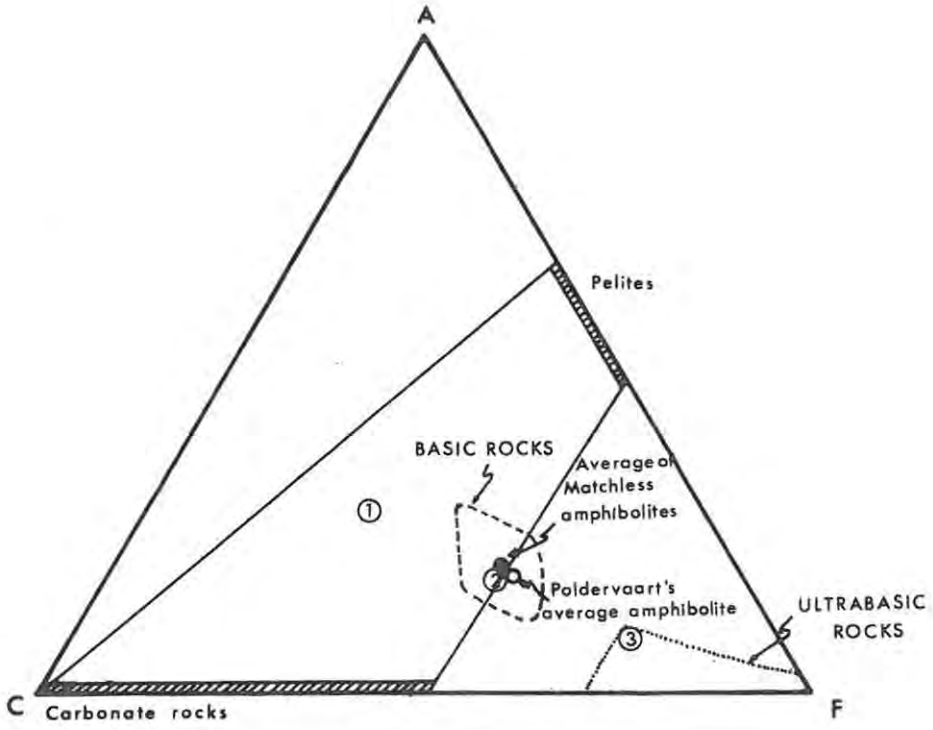

Figure 10. ACF diagram showing plot of various amphibolites relative to sedimentary and igneous fields (after Orville, 1969).

(1) Epidote amphibolite
(2) Porphyroblastic amphibolite
(3) Chlorite-amphibole schist

Ni are the most useful trace elements in distinguishing igneous from sedimentary trends since in the differentiation of igneous rocks, a decrease in mg is accompanied by a decrease in these trace elements. Plots showing a positive correlation between Niggli mg and Cr and Ni, indicative of control by igneous crystallisation, are shown in Figure 11. The departure of Ni in the talc schists from the expected trend is thought to be due to the high mobility and subsequent loss of nickel during alteration (Hawkes & Webb, 1962).

The trace element abundances for the amphibolites and talc schists are presented in Table 10. These values show some systematic variation. Ni, Cr and Co show a tendency to decrease with increasing differentiation, i.e. from ultrmafic talc schists, through chlorite-amphibole schists and porphyroblastic amphibolites to epidote amphibolite, whilst a corresponding enrichment in Sr and, to a lesser extent, Zr is clear. Nb is uniformly low and Ba values are erratic, possibly due to the high mobility of Ba during metamorphism (Philpotts, 1969). Rb contents are extremely low. The K/Rb ratios of the amphibolites range from 57 to 298 and average 149. The average Rb/Sr ratio in mafic and intermediate igneous rocks has been shown to be generally below 0.27 whereas shales and marls are greater than 0.47 due to enrichment of Rb relative to Sr during weathering (Faure & Powell, 1972, p. 6). The average Rb/Sr ratio of 0.20 for the Matchless Amphibolites further points to an igneous origin for these amphibolites.

Lithotype	Epidote Amphibolite				Porphyroblastic Amphibolite						Chlorite-amphibole Schist				Talc Schist			
Sample No.	SF49	SF59	SF69	SF84	SF73	SF74	SF75	SF77	SF82	SF83	SF85	SF14	SF16	SF76	SF81	SF1	SF3	SF80
Co	37	26	26	26	24	27	52	29	44	35	29	63	41	77	52	19	10	12
Ni	52	52	27	29	44	51	217	41	68	113	44	313	221	298	72	180	59	51
Cr	328	307	299	307	520	841	667	340	332	365	379	1039	1019	287	374	2394	1737	1847
Nb	19	21	21	11	13	20	17	17	25	22	19	13	10	16	27	10	10	10
Nb *	10	10		13	11					13			tr		19	tr		tr
Zr	125	144	145	139	137	128	133	132	155	133	104	75	48	101	172	28	10	10
Zr *	118	129		127	127					124			45		178	14		tr
Y	27	31	29	25	27	27	29	33	25	29	25	11	6	14	33	5	5	5
Y *	36	39		32	35					33			20		45	5		3
Rb	10	10	10	10	17	16	10	10	10	10	10	10	10	14	10	45	10	10
Rb *	tr	tr		tr	12					5			1		tr	31		3
Sr	313	370	497	359	191	180	66	124	124	141	162	10	10	21	78	67	11	10
Sr *	324	384		380	203					146			7		82	56		3
Ba	295	51	12	10	340	371	10	66	10	293	40	10	10	10	24	10	10	10
K/Rb	n.d.	n.d.	n.d.	n.d.	165	145	n.d.	n.d.	n.d.	293	n.d.	n.d.	80	57	n.d.	55	n.d.	26
Rb/Sr	n.d.	n.d.	n.d.	n.d.	0,089	0,088	n.d.	n.d.	n.d.	0,034	n.d.	n.d.	0,142	0,666	n.d.	0,671	n.d.	1
Zr/Nb	6,5	6,8	6,9	12,6	10,5	6,4	7,8	7,7	6,2	6,0	5,4	5,7	n.d.	6,3	6,3	n.d.	n.d.	n.d.

Analyst : General Superintendence Co., Johannesburg.

* : Duplicate determinations on pressed powder discs by S.H. Finnemore.

n.d. : Not determined.

Table 10. Trace element analyses of 15 Matchless amphibolites and 3 talc schists.

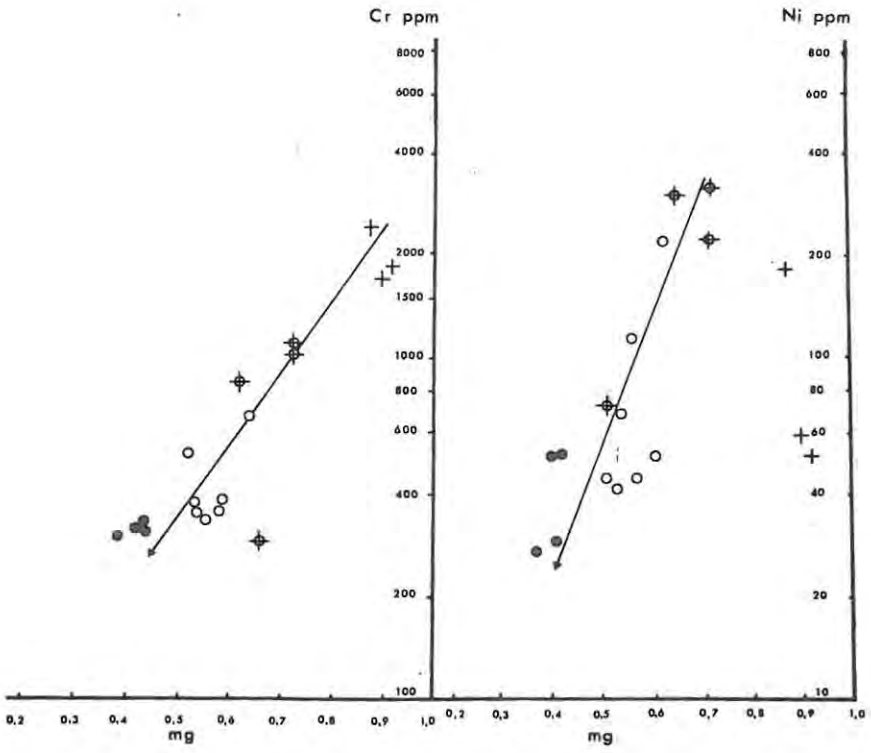

Figure 11. Plots of Cr and Ni ppm against Niggli mg for Matchless amphibolites and talc schists (modified after Kalsbeek and Leake, 1970). Symbols same as in Figure 8.

5.3. Origin of the Amphibolites and Talc Schists

The foregoing presentation shows that the Matchless amphibolites are igneous in origin. It remains to be seen to what association these rocks belong and whether they were derived from intrusive or extrusive material.

A few of the systematic changes in the major and trace element abundances of the Matchless rocks are illustrated in Figures 9, 11, 14 and 15 and Tables 8 and 10. The systematic changes in trace-element geochemistry are similar to the trace-element trends in the Skaergaard intrusion (Carmichael, Turner and Verhoogen, 1974, p. 480) where Cr, Ni and Co are removed early through the formation of pyroxenes, olivine and iron-oxide minerals. Sr is enriched as far as the lower part of the exposed layered series and there is a steady concentration of Ba, Rb and Zr in the last residual liquids while Ti is removed late during the formation of the titanomagnetite.

When plotted on the variation diagram MgO-CaO-Al_2O_3 (Fig. 14) the chemical analyses follow the trend for normal tholeiites and picrites (Viljoen and Viljoen, 1969, p. 285). Reference to this diagram shows that Ca- and CO_2-rich epidote amphibolites do not follow the expected course of differentiation but plot to the left of the curve. This deviation can be accounted for by either of two processes:

(i) the epidote amphibolites represent a plagioclase cumulate derived from a melt more highly differentiated than the porphyroblastic amphibolites or

(ii) the epidote amphibolite group is the end member of the proposed differentiation suite and has been enriched in Ca either by the introduction of Ca and/or CO_2, accompanied by a loss in volastiles, or calcite-veining.

The position of the epidote amphibolites in Figure 14 rules out the formation of an olivine, clinopyroxene and orthopyroxene-rich cumulate but not the formation of a plagioclase-rich cumulate. The abundant amounts of epidote in these rocks could have been derived from such a source. The second possibility is supported by the fact that Zr/Nb (Table 10) and Ti/Zr (Fig. 15) ratios are reasonably constant, indicating uninterrupted systematic differentiation of the suite (Weaver et al, 1972). This conclusion is supported by the Cr vs mg and Ni vs mg plots in Figure 10. Ca-metasomatism (and introduction of CO_2) accompanied by a loss of Na_2O, K_2O and SiO_2 or calcite veining could produce an epidote amphibolite of the required composition. This idea of late (and post-tectonic) metasomatic alteration or veining is strengthened by the presence of calcite veins and post-tectonic porphyroblasts within the amphibolites plus the fact that the dolomite rhombs within the talc schists are thought to have formed by this mechanism (see section 4.3.2.).

The average composition of the 15 Matchless amphibolites analysed is similar to Poldervaart's (1955) average for 200 amphibolites and representative olivine tholeiites and tholeiites (Carmichael, Turner and Verhoogen, 1974, p. 33)(Table12). The implication that the Matchless rocks are tholeiitic in composition is doubtful as the bulk composition of the amphibolites is not diagnostic of the parentage of these rocks. A truer reflection of the nature of the original magma is given by the

Lithotype	Epidote Amphibolite			Porphyroblastic Amphibolite							Chlorite-amphibole Schist					Talc Schist		
Sample No	SF49	SF59	SF69	SF84	SF73	SF74	SF75	SF77	SF82	SF83	SF85	SF14	SF16	SF76	SF81	SF1	SF3	SF10
q	12,20	17,40	n.d.	17,91	3,66	0,08	-	0,94	0,16	4,05	-	-	-	-	-	21,33	19,3	12,98
or	0,65	0,47	n.d.	0,77	2,01	1,65	0,71	1,54	0,83	1,06	2,01	0,06	0,06	0,06	0,71	1,77	0,06	0,06
ab	6,01	2,88	n.d.	3,30	25,47	22,59	7,78	26,40	28,26	25,21	25,55	1,69	2,96	2,12	17,60	1,27	0,25	0,93
an	34,77	35,40	n.d.	32,66	29,36	29,92	27,99	23,24	24,90	18,95	27,71	26,82	17,42	22,32	29,30	1,82	0,14	0,11
di en	8,34	9,86	n.d.	8,43	2,22	3,75	1,92	4,63	1,47	-	4,30	2,06	7,88	1,19	0,53	2,93	-	-
di fs	7,00	1,82	n.d.	1,56	1,02	1,38	0,73	2,34	0,77	-	1,84	0,28	2,67	0,54	0,69	0,72	-	-
di wo	11,41	13,01	n.d.	11,12	3,46	5,55	2,87	7,41	2,38	-	6,60	2,93	11,47	1,86	0,86	4,02	-	-
hy en	3,17	1,99	n.d.	1,73	13,77	17,59	25,44	14,60	18,90	20,25	13,78	20,33	31,75	29,42	23,10	25,89	56,67	70,41
hy fs	0,76	0,37	n.d.	0,32	6,32	6,47	9,70	7,35	9,87	10,55	5,90	6,80	10,78	13,30	12,07	6,35	8,10	7,83
fo	-	-	n.d.	-	-	-	5,59	-	-	-	1,60	19,27	3,84	8,10	0,67	-	-	-
fa	-	-	n.d.	-	-	-	2,35	-	-	-	0,76	7,11	1,44	4,04	0,38	-	-	-
mt	7,89	8,42	n.d.	7,37	4,68	3,77	5,35	4,47	4,07	3,12	4,36	2,90	3,28	3,74	4,99	0,68	0,17	0,19
il	3,04	3,36	n.d.	3,29	3,44	3,08	3,42	3,25	4,21	3,34	2,97	2,22	1,22	2,61	4,71	0,02	0,02	0,04
cc	6,75	2,32	n.d.	9,13	2,34	1,58	2,25	1,45	1,01	7,39	0,11	0,14	0,28	5,07	0,11	-	-	-
ap	1,47	0,95	n.d.	1,09	0,59	0,59	0,54	0,57	0,83	0,57	0,54	0,50	0,52	0,52	0,78	0,57	0,09	0,02
dl	-	-		-	-	-	-	-	-	-	-	-	-	-	-	26,71	9,64	1,14
c	-	-		-	-	-	-	-	-	2,92	-	-	-	-	-	-	0,60	0,39

n.d. = not determined

Table 11. C.I.P.W. weight percent normative compositions of Matchless metabasites.

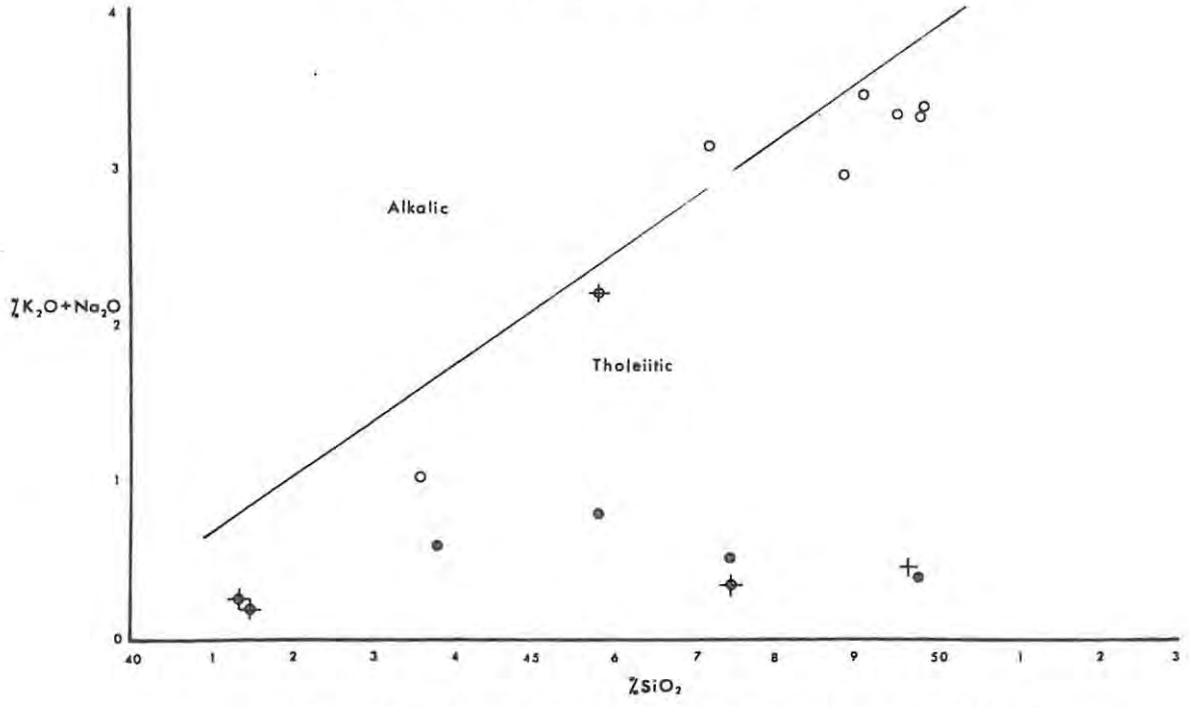

Figure 12. Plot of a Kuno ($Na_2O + K_2O$) versus SiO_2 diagram outlining the fields of alkali and tholeiitic basalts (after MacDonald and Katsura, 1964, p. 87).

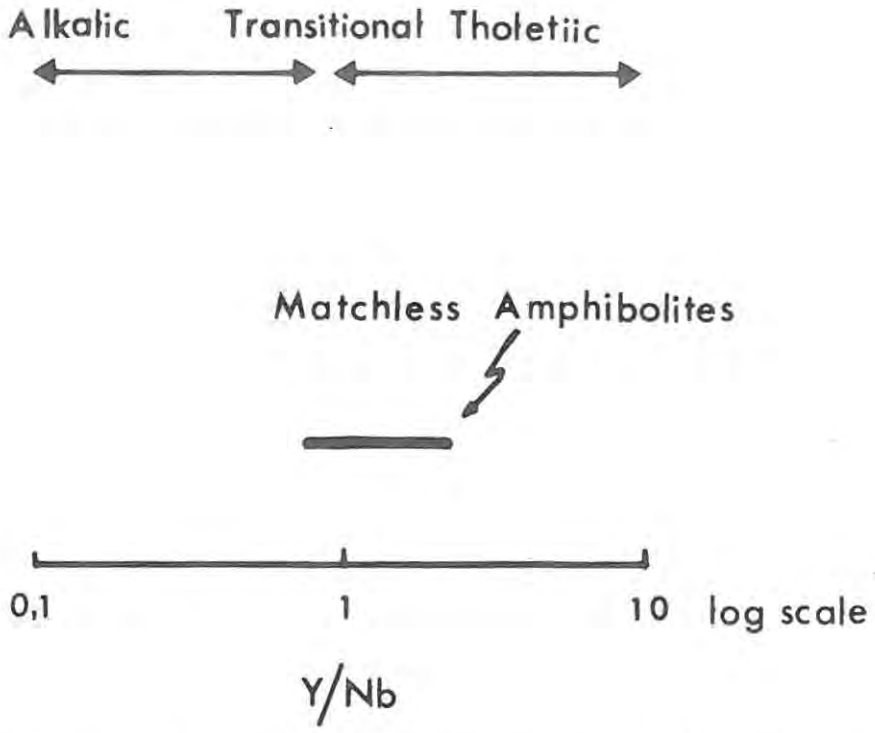

Figure 13. Plot of Y/Nb ratios showing position of Matchless amphibolites (after Pearce and Cann, 1973).

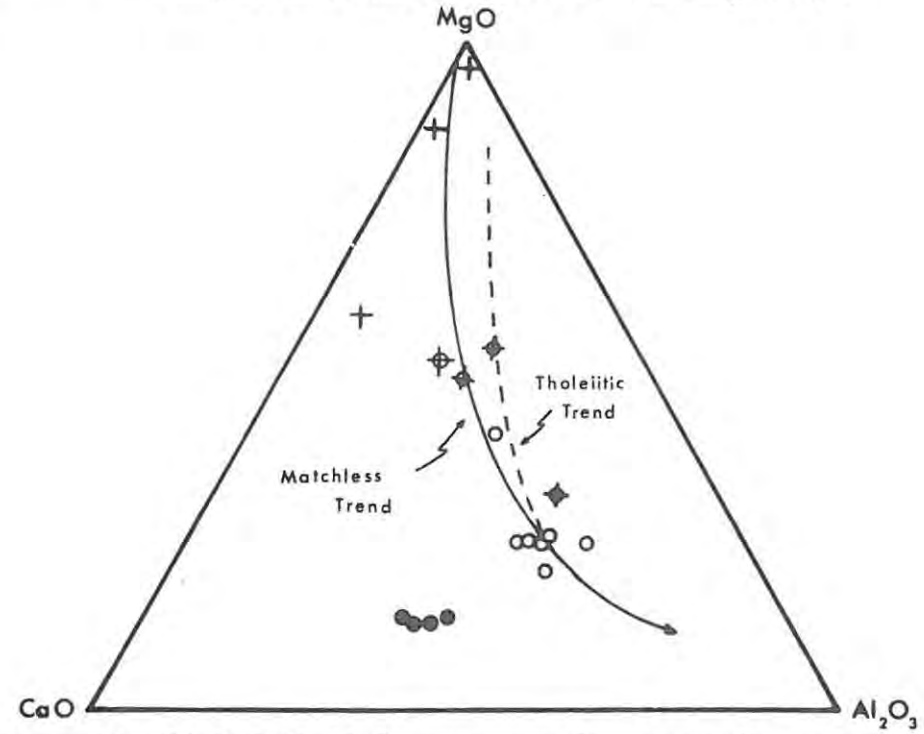

Figure 14. MgO-CaO-Al_2O_3 variation diagram indicating tholeiitic trend of Matchless basic and ultrabasic rocks (modified from Viljoen and Viljoen, 1969, p. 285). Symbols as in Figure 8. Differentiation trend of normal tholeiites - - - ; and Matchless rocks ——.

normative composition (Table 11) and Figures 12, 13 and 14 which illustrate the trends of variation of certain critical elements.

It is clear from the norms of the analysed amphibolites, using the criteria of Yoder and Tilley (1962, p. 354), that the original magma must have been of tholeiitic character with substantial normative orthopyroxene and small amounts of olivine presuming isochemical metamorphism. The absence of nepheline in the norms shows that the magma was not of alkali olivine basalt type according to Yoder and Tilley's (1962) definition. Plots of (K_2O + Na_2O) versus SiO_2 and Y/Nb ratios shown in Figures 12 and 13 both indicate that the Matchless amphibolites are tholeiitic in composition. This conclusion is supported by the plot of a MgO-CaO-Al_2O_3 variation diagram (Fig. 14) showing the tholeiitic trend (Viljoen and Viljoen, 1969, p. 285) and a similar trend for the Matchless amphibolites.

Table 12. Average compositions of amphibolites and various basic igneous rocks.

	1	2	3	4
SiO_2	46,34	50,3	47,01	51,57
TiO_2	1,65	0,6	3,20	0,80
Al_2O_3	12,78	15,7	15,57	15,91
Fe_2O_3	3,71	3,6	2,32	2,74
FeO	7,93	7,8	11,57	7,04
MgO	9,78	7,0	5,25	6,73
CaO	11,27	9,5	9,77	11,74
MnO	0,23	0,2	0,20	0,17
Na_2O	1,31	2,9	3,00	2,41
K_2O	0,13	1,1	0,31	0,44
P_2O_5	0,33	0,3	0,32	0,11
CO_2	1,56			
H_2O^-	0,13		1,64	0,45
H_2O^+	2,53			
Total	99,68	100,00	100,16	100,11
Ox ratio	29,51	29,40	nd	nd

1. Average 15 Matchless amphibolites
2. Average of 200 amphibolites. Water free (Poldervaart, 1955, p. 136)
3. Olivine tholeiite (McBirney and Williams, 1968, in Carmichael et al, 1974)
4. Tholeiite (Lowder and Carmichael, 1970, in Carmichael et al, 1974).

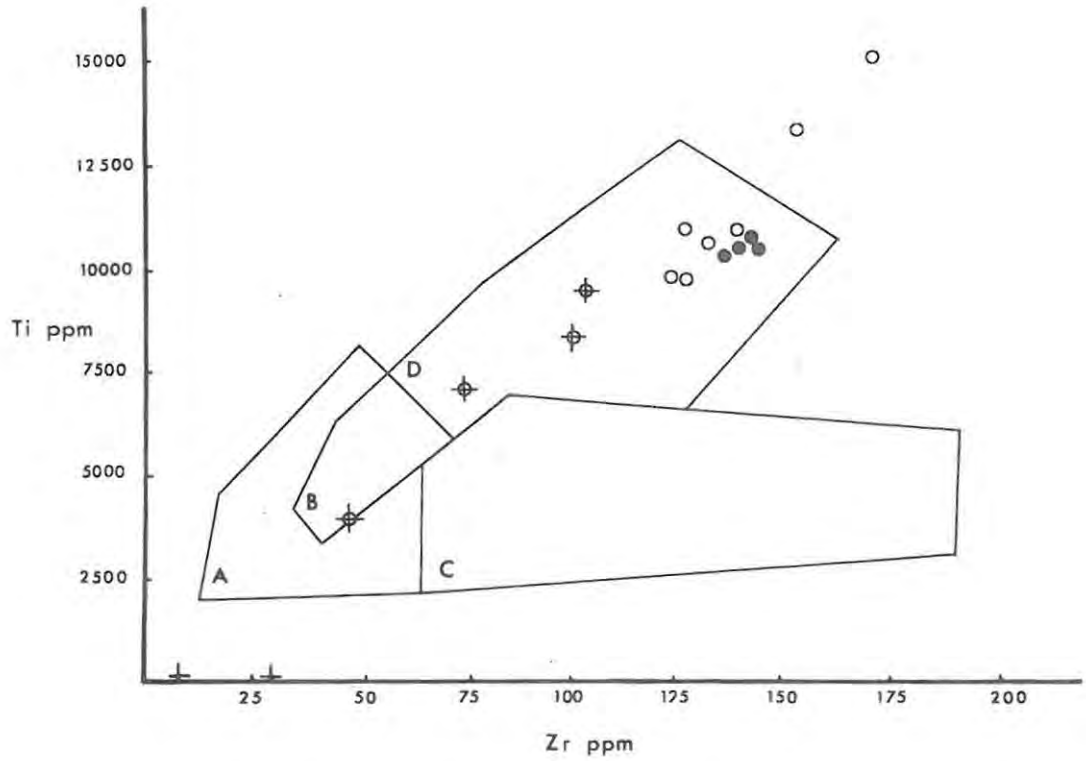

Figure 15. Ti versus Zr (after Pearce & Cann, 1973) Fields: D and B - ocean floor basalts; C and B - calc-alkali basalts; A and B - low potassium tholeiites.

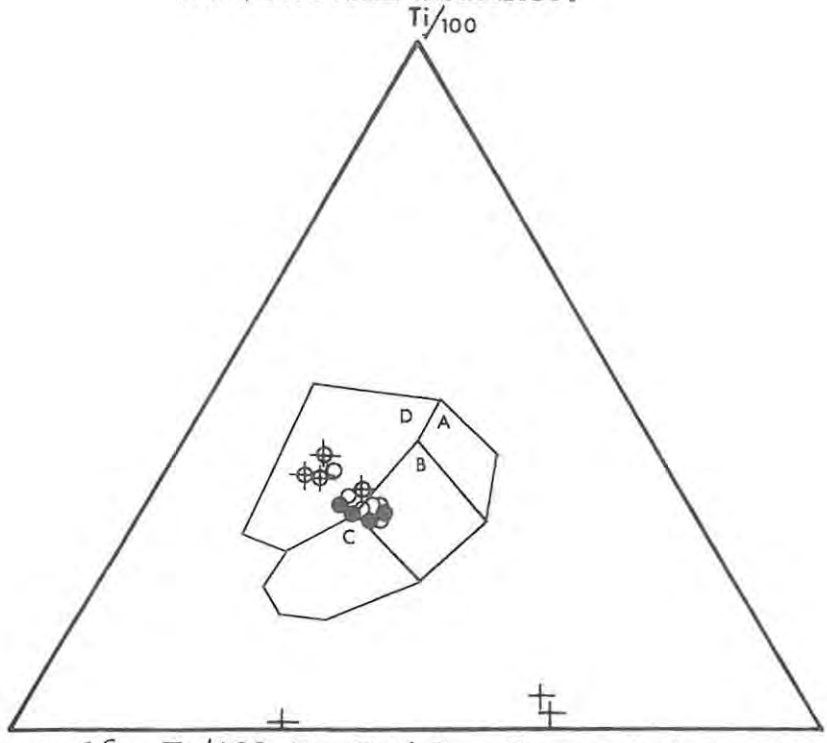

Figure 16. Ti/100-Zr-3Y (after Pearce & Cann, 1973) Fields: D - "within-plate" basalts; C and B - calc-alkali basalts; B - ocean floor basalts; A and B - low potassium tholeiites.

Utilization of the trace element data has yielded information regarding the tectonic setting of the tholeiitic magma. Pearce and Cann (1973) have used analyses for Ti, Nb, Zr, Y and Sr in over 200 basaltic rocks to construct diagrams in which the tectonic setting of basalts can be identified. They suggest that, of these elements, Ti, Nb, Zr and Y are insensitive to processes of alteration and low-grade metamorphism whereas Sr is unsatisfactory since it is only stable in uncarbonated rocks below greenschist facies metamorphism. The diagrams used in this study to discriminate visually between their four magma types (ocean floor basalts, volcanic arc basalts, ocean island basalts, continental basalts) will be Ti-Zr and Ti/100-Zr-3Y.

It is clear from the Ti-Zr plot illustrated in Figure 15 that, besides a positive correlation between Ti and Zr possibly indicating control by igneous differentiation, the bulk of the Matchless amphibolites falls in the field of the ocean floor basalts. The data in Figure 16 are not conclusive since the plots straddle the boundary between the ocean floor basalts and "within-plate" basalts, yet is apparent from these two figures that the Matchless metabasites could represent one of the following groups of igneous rock:

(i) tholeiitic ocean floor basalt (at diverging plate margin)

(ii) tholeiitic ocean island or continental basalt ("within-plate" basalt).

Miyashiro (1975), who uses the term "abyssal tholeiite" in preference to "oceanic tholeiite" which has been used by some authors to include tholeiites of both ocean floors and oceanic islands, states that Pearce and Cann's (1973) diagrams have no diagnostic value in the determination of the origin of these rocks since their fields of ocean-floor basalts actually contain many points of island arc basalts. Miyashiro (1975) believes that consideration of the variation of trace element contents of rocks in relation to the advance of fractional crystallisation (or to increasing FeO*/MgO) is a more effective use of the trace element data. A plot of Ni versus FeO*/MgO (not included in the text) did not reveal any further information on the tectonic setting and origin of the Matchless metabasites. However, comparison of the major element data shown in Table 12 indicates that the Matchless rocks and abyssal tholeiites have similar chemical compositions. The wider range in Matchless compositions could be due to differentiation with the formation of cumulative rocks (talc schists) and some late differentiates (epidote amphibolites).

Pearce, Gorman and Birkett (1975) have used the ternary diagram TiO_2-K_2O-P_2O_5 as a method of discriminating between oceanic and non-oceanic (continental) basalts. The Matchless rocks qualify for use on this diagram in that they have total alkalies $\leq$ 20% in an (Fe_2O_3 + FeO)-MgO-(Na_2O + K_2O) diagram. Reference to Figure 16 indicates that all the Matchless basic and ultrabasic rocks fall above the dividing line, within the oceanic basalt field. Pearce, Gorman and Birkett (1975) state that metamorphosed oceanic basalts will tend towards K_2O enrichment and leave the oceanic field in the TiO_2-K_2O-P_2O_5 diagram. As a corollary, they infer that if a metamorphosed basalt falls within the oceanic field of the diagram, it is very likely to be of oceanic origin. Besides this the chemical properties of the Matchless amphibolites are similar to the distinctive pattern of oceanic tholeiites in that they are very low in K_2O and TiO_2 and have low total iron and P_2O_5 and high Ca (Carmichael et al,

Table 13. Usual ranges of compositions of tholeiitic (TH) series volcanic rocks in different settings (after Miyashiro, 1975) compared with range of compositions of Matchless basic rocks.

	Island arcs, TH series	Mid-oceanic ridges, Abyssal tholeiites	Oceanic islands TH series	Matchless Amphibolites
FeO*/MgO	1 - 7	0,8 - 2,1	0,5 - 2,5	0,63 - 2,60
SiO_2 %	46 - 47	47 - 51	45 - 65	41,35 - 49,88
FeO* %	6 - 16	6 - 14	8 - 16	9,07 - 14,77
Na_2O %	1,1 - 3,6	1,7 - 3,3	0,7 - 4,5	0,20 - 3,34
K_2O %	0,1 - 2,0	0,07 - 0,40	0,06 - 2,0	0,01 - 0,34
TiO_2 %	0,3 - 2,0	0,7 - 2,3	0,2 - 5,0	0,65 - 2,51

FeO* = total iron as Feo.

1974, 376-377, analyses 1-5). K/Rb is exceptionally high (700 to 1700) in oceanic tholeiites but not in the Matchless rocks which, where calculated, range between 26 and 293 (Table 10). The comparison of CaO/Al_2O_3 ratios is not made because of possible post-tectonic Ca-metasomatism of some of the amphibolites.

If the Matchless basic and ultrabasic suite could be considered to be ophiolitic, it would fall into Miyashiro's (1975) Class II of ophiolites, that is, a class characterised by volcanic rocks only of the TH series. However, the chemical composition of the Matchless metabasites is not unlike that of the Sanbagawa basic schists (Tatsumi, 1970) which belong to Class III, a class characterised by the presence of both TH and alkalic series of volcanic rocks.

It is obvious from the aforegoing discussion that the Matchless rocks have definite affinities with oceanic tholeiites however, until more is known about the role of plate tectonics in the formation of the Damara belt, speculation regarding the origin of the oceanic material will be rather tenuous.

It is generally believed (Viljoen in Anhausser and Button, 1974) that the Matchless suite represents a horizon of basic volcanic rocks. No definite proof of this origin has been published besides Hälbich's (1970, p. 56) observation that amygdales are present in less sheared and metamorphosed amphibolites lower in the Khomas sequences than the Matchless amphibolites. Elliott and Cowan (1966) in a study of the amphibolites of the Holleindaler Greenstone Group, Jotunheimer, Norway, have differentiated between extrusive and intrusive basic rocks on the basis of oxidation ratios. If it is assumed that the oxidation ratios are inherited from the parent igneous material (Eliott and Cowan, 1966, p. 323), it is logical to conclude from the data in Table 14 that all three types of Matchless amphibolite were originally extrusive.

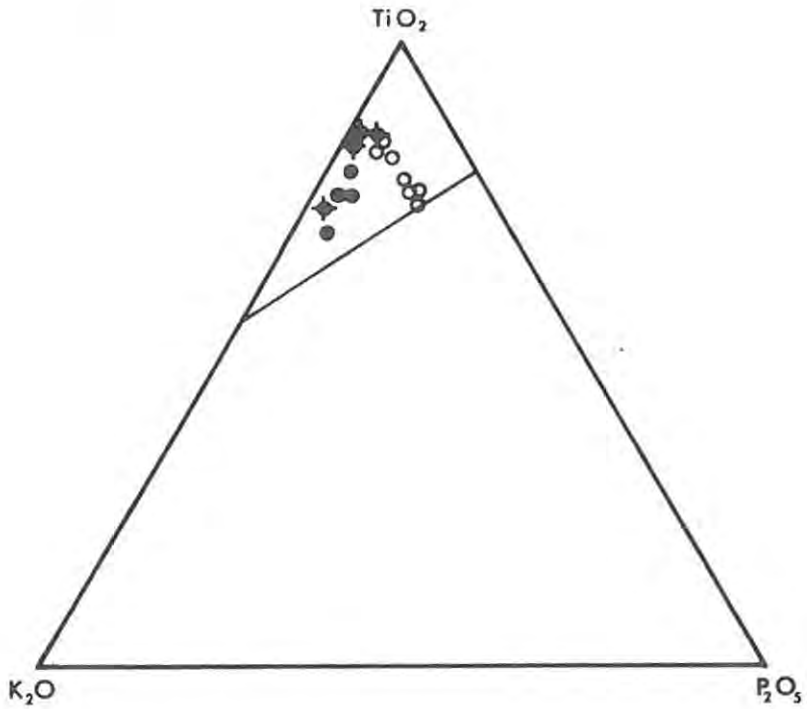

Figure 17. TiO_2-K_2O-P_2O_5 plot of Matchless basic rocks, showing the dividing line between the oceanic field (upper portion) and non-oceanic field (lower portion)(after Pearce, Gorman and Birkett, 1975). Symbols as in Figure 8.

Table 14. Oxidation ratios, mol $\frac{2Fe_2O_3 \times 100}{2Fe_2O_3 + FeO}$ of intrusive and extrusive basic igneous rocks (after Elliott and Cowan, 1966). *Ox. ratios calculated only for diamond-drill core samples.

	Fe_2O_3	FeO	Ox. Ratio
Average Palisades dolerite	1,6	8,7	14,2
Average Watchnung basalt	3,4	8,6	26,1
Average Spitzbergen intrusives	3,4	10,3	22,7
Average Spitzbergen extrusives	4,8	10,1	30,0
Average Karoo basic intrusives	1,2	9,3	11,0
Average Karoo basic extrusives	2,7	7,9	23,6
Average of above intrusives	2,1	9,4	16,5
Average of above extrusives	3,6	8,9	26,8
Average of Matchless epidote amphibolites*	5,6	4,9	68,7
Average of Matchless porphyroblastic amphibolites*	2,9	8,0	42,0
Average of Matchless chlorite-amphibole schists*	2,5	10,8	32,1

Finally, it is concluded:

(i) The amphibolites and talc schists are of igneous origin and form part of a differentiated series

(ii) The rocks have affinities with oceanic tholeiites

(iii) On the assumption that the oxidation ratios are inherited they are considered to represent extrusive basic rocks.

6. ECONOMIC GEOLOGY

6.1. Copper deposits associated with the Matchless Amphibolite Belt.

A number of stratabound copper-pyrite deposits have been proved along the Matchless amphibolite belt within the Khomas succession of the Damara orogen. The amphibolite belt consists of a zone of conspicuous amphibolitic rocks, up to 3 km wide, which strikes ENE for a distance of 300 km, parallel to the trend of the Damara orogen. The belt is made up largely of bands and lenses of amphibolite, amphibolitic schist and talc schist, and is often accompanied, along strike, by lenses of sericitic quartzite, all lying within isoclinally folded Khomas schists of the Damara Supergroup.

The main copper occurrences associated with the belt are at Otjihase Mine, 20 km northeast of Windhoek, Matchless Mine, 30 km southwest of Windhoek, and at the Gorob and Hope mines in the Namib Desert Park, about 225 km southwest of Windhoek (see Figure 18). Mineralisation of importance is also known from a number of other localities.

6.1.1. Otjihase Mine

The Otjihase deposit lies on the farm Von Francois Ost 60 and outcrops ~300 m north of units of the Matchless amphibolite belt conformably within shallow, northwards-dipping Khomas schists, in the hangingwall of the amphibolites. A northern belt of amphibolite is also present commencing just east of the Otjihase gossan where it is associated with a number of distinctive talc, chlorite-carbonate rocks, which continues eastwards as a zone of discontinuous and scattered amphibolite lenses (Viljoen et al, 1975). Exploration has indicated ore reserves of 16 million tons to a depth of 400 m with an average grade of 2,25% copper. In addition the ore contains a lower percentage of zinc in sphalerite and a small amount of silver associated with chalcopyrite (Anonymous, 1973).

The mineralisation at Otjihase is confined to discrete, well-defined tabular masses of siliceous, cherty and/or quartzitic rock (M.J. Viljoen reported in Anhausser and Button, 1974). Pyrite is the main sulphide and occurs as disseminated and massive beds and layers within the quartzite assemblage. The ore body can be divided into four separate "shoots" or "lenses" on criteria of metal content and grade (Vellet, written communication). The northernmost shoot contains chalcopyrite and low-grade zinc values which cut out abruptly with depth to form two copper-rich shoots. The average copper value drops sharply where the shoot passes into zinc-free ore. A low-grade and narrow copper-rich shoot lies to the south of, and parallel to, the three northern shoots but is separated from them by 150 m of waste rock.

The ore body maintains a regular northeast strike and a northwest plunge of 16°. Regionally, the amphibolite and surrounding sediments show a consistent northwesterly dip of between 20° and 30°. Reference to the geological map (Map 1) indicates that north-trending, west-dipping faults, which are downthrown in the west, cut the Otjihase body at its northwestern extremity. Mapping indicates that the mineralised horizons are not continuous and crop out irregularly over a strike length of

approximately 500 m. The trace of the ore horizon on surface is given by both a red gossanous schist and a quartzitic layer carrying vugs of limonite and in places chrysocolla and malachite (Vellet, written communication). The quartzite and footwall schists contain magnetite in places. Surface observations show that oxidation of pyrite is responsible for most of the gossan.

6.1.2. Matchless Mine

Matchless Mine is situated on the farm Friedenau 16 in the Khomas Highlands, 30 km southwest of Windhoek. The ore body lies within Khomas schists and sericitic quartzites underlying the amphibolite belt. Like Otjihase, the ore is confined to discrete, well-defined tabular masses of quartzitic rock. Approximately 3 million tons of ore with a grade comparable to Otjihase have been proved down to a depth of 375 m.

The copper-pyrite ore zone consists of several shoots arranged "en echelon" which are parallel to l_2 lineations and B_2 lineations and B_2 fold axes (Hälbich, 1970). The horizontal projection of the ore body strikes due west and plunges at 23° in that direction.

Hälbich (1970) states that single pyrite grains commonly unite to form composite aggregates that extend parallel to the s_2-schistosity. Pyrite and chalcopyrite occasionally deviate from the schistosity and grow

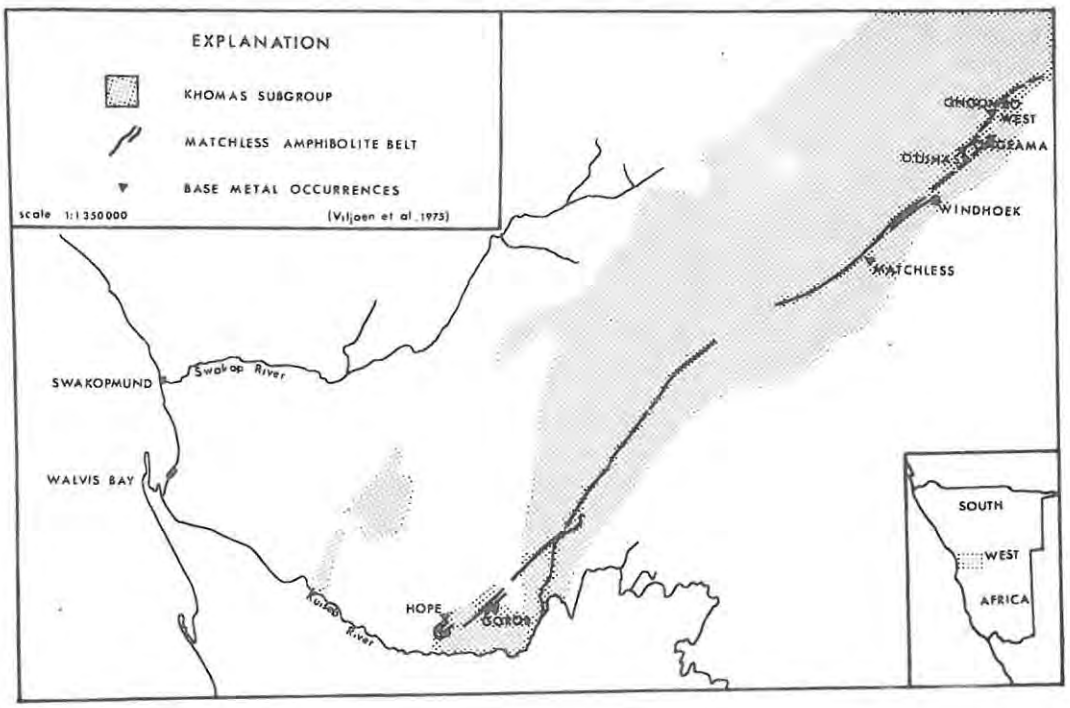

Figure 18. Some of the copper deposits associated with the Matchless Amphibolite Belt in the Damara Orogen, S.W.A.

along the s_3-cleavage. Furthermore, he states that there is a scarcely-perceptible elongation on the schistosity of patches of pyrite parallel to the lineation l_2 which indicates that the sulphide ores were affected together with the country rocks in the regional deformation.

6.1.3. Gorob and Hope Mines

The old Gorob and Hope mines are situated at the folded WSW extremity of the belt within the Namib Desert Park. According to Wagner (1916), steeply dipping mica schists which enclose a series of lenticular masses of quartzite, are strongly "impregnated" with copper mineralisation just above the quartzites. Similar conditions prevail at the Hope Mine with the mineralisation being confined to three more or less continuous zones of mica schist with a combined length of 120 m. The ore at depth is chalcopyrite and pyrite and is replaced on surface by malachite, chrysocolla, cuprite and limonite. Although not mentioned by Wagner (1916), these deposits are believed to be related to the amphibolite belt and to have a similar mineralogy, grade of mineralisation and geological setting to that of the Otjihase and Matchless deposits (Vellet, personal communication).

6.2. Common features of the deposits

The copper-pyrite deposits found along the belt vary in size but are essentially similar to one another in their mode of occurrence, shape, mineralogy and ore texture and have the following common characteristics:

(i) The deposits occur in the hangingwall or footwall of units of the Matchless amphibolite belt.

(ii) The mineralisation is associated with tabular masses of siliceous, cherty and/or quartzitic rock.

(iii) The ore bodies are lenticular in form and lie conformably within crystalline, isoclinally-folded, semi-pelitic and basic schists.

(iv) They are composed mainly of massive compact ores consisting of pyrite with chalcopyrite, some sphalerite and pyrrhotite.

(v) Both the ores and the enclosing country rocks have been subjected to three phases of deformation.

6.3. Comparison with other cupreous - pyrite deposits

The Matchless belt deposits are similar to the Besshi-type copper pyrite deposits of the Sanbagawa belt in western Japan (Kanehira and Tatsumi, 1970). The common features and similarities of these types of deposits are listed below:

(i) Both the Besshi and Matchless type deposits are conformable with the surrounding crystalline, isoclinally-folded, schists of basic and pelitic origin and are accompanied by quartzose rocks.

(ii) The deposits are tabular in form and are associated with

metamorphosed basic volcanics.

(iii) The sulphides are classified into three types; compact ore, banded ore and copper-rich ore. The compact ores consist chiefly of pyrite, chalcopyrite sphalerite and a small amount of gangue minerals, the banded ore is a mixture of sulphides and silicates, and the copper-rich ore is essentially a mixture of chalcopyrite and minor pyrite and gangue minerals.

(iv) Compositional banding is found in the compact ore and schistosity is conspicuous in the banded ore.

(v) Magnetite-quartz schist occurs in thin layers in either the hangingwall or footwall of the ore bodies.

(vi) The basic schists accompanying the Besshi copper-pyrite deposits are chemically similar (Kanchira and Tatsumi, 1970, p. 56) to the Matchless amphibolites and resemble oceanic tholeiites.

The miocene Kuroko ore deposits frequently occur near rhyolitic domes and explosion breccias and are made up of layers of sphalerite-galena-barite and pyrite-chalcopyrite. These deposits are mineralogically dissimilar to the Matchless belt deposits and because of this, and the fact that they are associated with felsic, calc-alkaline volcanic rocks (Hutchinson, 1973), will not be compared with the Matchless belt deposits.

The Cyprus deposits, which lie at various levels near the top of a sequence of pillowed basic lavas,occur as massive stratiform pods of pyrite containing a few percent chalcopyrite, or as disseminated irregular or pipe-like pyritic replacements of brecciated pillow lava or volcanic breccia lenses (Clark, 1970). The Cyprus and Matchless ore deposits are mineralogically similar and are both associated with lavas that resemble modern oceanic tholeiites, however, unlike the Matchless belt, the sedimentary rocks associated with the Cyprus deposits are volumetrically insignificant (Hutchinson, 1973). Both deposits are associated with chemically deposited radiolarian cherts and ironstones.

The Matchless belt deposits belong to Hutchinson's (1973) third type of volcanogenic massive base metal sulphide deposit, namely, the cupreous pyrite type. These deposits, which include the Cyprus deposits, contain virtually no lead, only minor zinc and are associated with igneous rocks of mafic-ultramafic composition and of ophiolitic affinity.

6.4. Origin of the deposits

The massive cupreous-pyrite sulphide deposits associated with the Matchless amphibolite belt are volcanogenic in origin and are believed to have been formed subaqueously by volcanic-fumarolic activity. This type of deposit, which belongs to Hutchinson's third type massive sulphide deposit, is believed by him to be the product of relatively deep water, quiescent, fissure eruptions presumably like those occurring along modern oceanic rift-ridge systems. The abundance of sedimentary rocks within the Khomas subgroup suggest however, that a landmass existed nearby during the time of formation of the Matchless belt and that extrusion

of the Matchless suite was unlikely to have taken place in a deep ocean basin. It is more likely that the origin of the Matchless belt deposits is similar to that of the Besshi-type deposits which are believed by Tatsumi et al (1970) to have formed during submarine eugeosynclinal volcanic activity. The formation of these deposits in "in situ" orogenic belts has been demonstrated by Bilibin (1967) to have taken place during the initial and early stages of eugeosynclinal development. The magnetite quartzite and other siliceous horizons (e.g. quartzite, sericitic quartzite) associated with the ore deposits probably represent chemically deposited radiolarian cherts and ironstones.

The wide acceptance that stratiform massive sulphide deposits, consisting of pyrite and/or pyrrhotite, with various amounts of chalcopyrite, sphalerite and galena, are genetically related to submarine volcanism in so-called "eugeosynclinal" environments has recently been reinterpreted by Sillitoe (1972) in terms of the theory of plate tectonics. He suggests that many cupriferous massive sulphide deposits are temporally and spatially related to the tholeiitic basalts which constitute layer 2 of the oceanic crust and are transported away from the ocean rises by means of sea-floor spreading. On reaching the margins of the ocean basins, the massive sulphide deposits are under thrust along subduction zones beneath continental margins and island arcs. During subduction, some of the deposits are incorporated mechanically into the continental crust as parts of slices of oceanic lithosphere.

The available published evidence for the Damara (Clifford, 1968; Shackleton, 1969, 1973; Hurley, 1972) is more in favour of an ensialic "in situ" orogeny rather than a collision-type orogeny and, although the Matchless basic and ultrabasic rocks have affinities with oceanic tholeiites and could possibly be termed ophiolitic, it is believed that insufficient is known of the role of plate tectonics in the formation of the Damara orogen to permit the application a plate tectonic model to the origin of the cupreous-pyrite deposits.

7. CONCLUSIONS

The Elisenheim area is situated within the Windhoek Formation in the southern portion of the Damara Orogen. The property is underlain by a monotonous succession of quartz biotite schists and micaceous "quartz-augen" schist with intercalations of amphibolite, graphitic schist and marble. The most conspicuous of the intercalations is the Matchless Amphibolite which, on petrographic criteria, has been divided into three different rock-types, namely, epidote amphibolite, porphyroblastic amphibolite and chlorite-amphibole schist. Dolomitised talc schists outcrop in the extreme north of the property.

Deposition of the semi-pelitic sediments and extrusion of the tholeiitic basalts (marked by the Matchless Amphibolite) was followed by three periods of deformation. The F_1 phase is evident throughout the area as a deformed s_1-cleavage. Second phase deformation resulted in the transposition of pre-existing structures and gave rise, amongst other features, to the braided outcrop pattern of the amphibolite belt. Towards the end of this phase, B_3 crenulations were superimposed on the transposed s_2-schistosity in the more incompetent horizons. The generation of major north-trending, normal faults took place during this third phase (Hälbich, 1970).

Medium grade (Winkler, 1974) regional metamorphism accompanied the F_1, F_2 and F_3 phases of deformation and outlasted the F_3 phase. Mineral assemblages throughout the area are those of amphibolite facies and are indicative of a single prolonged period of metamorphism. Textural studies show that garnet, biotite and hornblende metamorphism outlasted deformation. The P,T conditions prevailing during metamorphism are estimated to be at least 5 kb at $\sim$550°C.

The complex zonal and patchy intergrowths of hornblende and actinolite are believed to have resulted from non-equilibration during pro-grade metamorphism.

Petrochemical evidence indicates that the three amphibolite types and talc schists are genetically related and that they form a possible differentiation sequence. The original magma was tholeiitic in character and displays oceanic affinities. Oxidation ratios suggest that the amphibolites are derived from an extrusive sequence, which, by virtue of its association with semi-pelitic sediments and massive cupriferous pyrite ore deposits typically produced during submarine vulcanicity, are thought to have been deposited subaqueously.

The Matchless amphibolites and sulphide ores have been deformed by F_1, F_2 and F_3 and metamorphosed to amphibolite facies indicating that they were deposited early in the Damara tectonic cycle and simultaneously with the similarly deformed and metamorphosed Khomas schists. Viljoen (reported in Anhausser and Button, 1974) considers that the clearly bedded nature of the deposits suggests that they belong to the class of eugeosynclinal submarine exhalative volcano-sedimentary deposits which have been shown by Bilibin (1967) to have formed in "in situ" orogenic belts during the initial and early stages of eugeosynclinal development.

Various writers (Sillitoe, 1972; Hutchinson, 1973) believe that

many massive cupreous-pyrite deposits, temporally and spatially associated with oceanic tholeiites, were generated at the ocean rises and were incorporated mechanically into the continental crust as parts of slices of oceanic lithosphere and cannot be interpreted as having formed during the initial stages of eugeosynclinal development. The application of this model for the origin of the Matchless amphibolites and associated copper deposits is debatable since the origin of Pan-African type orogenic belts, of which the Damara is an example, has been ascribed to "in situ" large-scale upwelling and remobilisation of sialic material along zones of weakness within cratonic blocks (Clifford, 1968; Shackleton, 1969, 1973; Hurley, 1972) rather than to continental collision following plate movements and subduction of oceanic crust (Burke and Dewey, 1973). However, until more is known of the role of plate tectonics in the formation of the Damara belt, speculation regarding the origin of the Matchless basic and ultrabasic rocks and associated ore deposits according to a plate tectonic theory will be rather tenuous.

It therefore suffices to say that the Matchless metabasites and associated copper deposits were deposited in an elongated trough of sediments of probable eugeosynclinal type during the initial stages of development of the Damara orogen.

APPENDIX

Determinative Mineralogy

Modal compositions of the rocks were determined micrometrically on thin sections by means of a Swift automatic point counter. Point spacings were similar to the average grain size of the rocks and 1200 to 2000 counts per sample were found to be adequate. Refractive index determinations were made on various minerals separated from the specimen under a binocular microscope. If this was not practical, a small crush of the rock was found to be adequate. Standard immersion methods, using sodium light, were employed. The indices of refraction were checked after each determination on a Leitz-Jelly refractometer. Distinction between untwinned plagioclase and potassium feldspar was aided by the staining of the two phases pink and yellow respectively with cobaltinitrite and amaranth (Norman, 1974). The composition of plagioclase was determined on a universal stage by the Rittman zonal method i.e. measurement of the extinction α^1 to (010) in the zone [100] outlined by Chudoba and Kennedy (1933, p. 41). The rhombohedral carbonate porphyroblasts within the talc schists were identified by X-ray diffraction traces with the help of ASTM data cards as being composed of dolomite after staining with Cu $(NO_3)_2$ (Wolf, 1967) and immersion in HCI had failed to yield any positive results.

Whole-rock Chemical Analyses

Complete major-element and trace element (Ni, Co, Cr, Nb, Zr, Y, Rb, Sr and Ba) analyses of 20 samples were performed by X-ray fluorescence methods by the General Superintendence Company. Nb, Zr, Y, Rb and Sr were determined by the writer on 9 samples (49, 59, 84, 73, 83, 16, 81, 1, 80) by X-ray fluorescence techniques. Analyses were undertaken on pressed powder discs against standard samples GSP-1, BCR and OK-272 using a Philips PW 1540 manual spectrometer and PW 1130/90 generator.

REFERENCES

Anhausser, C.R., & Button, A. (1974) A review of southern African stratiform ore deposits - their position in time and space. Economic Geol. Res. Unit. Univ. Witwatersrand. Inf. Circ. 85, 48p.

Anonymous (1973) Go-ahead for Otjihase copper, South West Africa. Mining Mag., 129, 177-179.

Bilibin, Yu.A. (1968) Metallogenic provinces and metallogenic epochs. Geol. Bull., Queens College Press, Flushing, New York, 35p.

Brady, J.B. (1974) Coexisting actinolite and hornblende from west-central New Hampshire. Am. Mineralogist, 59, 529-535.

Burke, K.C. & Dewey, J.F. (1973) An outline of Precambrian plate development. In : Tarling, D.H. & Runcorn, S.K. (Eds.), Implications of continental drift to the earth sciences, 2. Academic Press, London, 1035-1045.

Carmichael, I.S.E., Turner, F.J., & Verhoogen, J. (1974) Igneous Petrology. McGraw-Hill Book Co., New York, 730p.

Choudhuri, A. (1972) Hornblende-actinolite and hornblende-cummingtonite associations from Cuyuni River, Guyana, South America. Am. Mineralogist, 57, 1540-1546.

_____ (1974) Distribution of Fe and Mg in actinolite, hornblende and biotite in some Precambrian metagraywackes from Guyana, South America. Contrib. Mineral. Petrol., 44, 45-55.

Chudoba, K., & Kennedy, W.Q. (1933) Feldspar determination. Thomas Murray & Co., London, 41p.

Clark, L.A. (1971) Volcanogenic ores; comparison of cupriferous pyrite deposits of Cyprus and Japanese Kuroko deposits. Soc. Mining Geol. Japan, Spec. Issue, 3, (IAGOD vol.) 206-215.

Clifford, T.N. (1968) Radiometric dating and the pre-Silurian geology of Africa. In : Hamilton, E.I. & Farquhar, R.M., Radiometric dating for geologists. Interscience, London, 299-416.

Cooper, A.R., & Lovering, J.F. (1970) Greenschist amphiboles from Haast River, New Zealand. Contrib. Mineral. Petrol., 27, 11-24.

Elliott, R.B., & Cowan, D.R. (1966) The petrochemistry of the Holleindalen Greenstone Group, Jotunheimen, Norway. Norsk. Geol. Tiddskr., 46, 309-326.

_____ (1973) The chemistry of gabbro/amphibolite transitions in South Norway. Contrib. Mineral. Petrol., 38, 71-79.

Engel, A.E.J., & Engel, C.G. (1962) Progressive metamorphism of amphibolite, northwest Adirondack Mountains, New York. In : Petrologic studies: a volume to honour A.F. Buddington.

Ernst, W.G. (1968) Amphiboles. Springer. Berlin., 152p.

Faure, G., & Powell, J.L. (1972) Strontium isotope geology. Berlin. Springer-Verlag., 188p.

Field, D., & Elliott, R.B. (1974) The chemistry of gabbro/amphibolite transitions in south Norway. II. Trace Elements. Contrib. Mineral. Petrol., 47, 63-76.

Gevers, T.W. (1934) The geology of the Windhoek district in South West Africa. Trans. Geol. Soc. South Africa, 37, 221-251.

Graham, C.M. (1974) Metabasite amphiboles of the Scottish Dalradian. Contrib. Mineral. Petrol., 47, 165-185.

Grapes, R.H. (1975) Actinolite-hornblende pairs in metamorphosed gabbros, Hidaka mountains, Hokkaido. Contrib. Mineral. Petrol., 49, 125-140.

Guj, P. (1967) Structural geology of the Auas mountains, Windhoek district, South West Africa. Annals. Geol. Surv. S. Afr., 6, 55-62.

Hälbich, I.W. (1970) The geology of the western Windhoek and Rehoboth districts: a stratigraphic-structural analysis of the Damara System. Unpubl. D.Sc. Thesis. Univ. Stellenbosch, 199p.

Hawkes, H.E., & Webb, J.S. (1962) Geochemistry in mineral exploration. Harper & Row, Publishers, New York, 415p.

Hess, H.H. (1933) The problem of serpentinization and the origin of certain chrysotile asbestos, talc and soapstone deposits. Econ. Geol. 28, 634-657.

Hurley, P.M. (1972) Can the subduction process of mountain building be extended to Pan-African and similar orogenic belts? Ear. Planet. Sci. Lett., 15, 305-314.

Hutchinson, R.W. (1973) Volcanogenic sulphide deposits and their Metallogenic significance. Econ. Geol., 68, 1223-1246.

Jacob, R.E. (1974) Geology and metamorphic petrology of part of the Damara Orogen along the lower part of the Swakop River, South West Africa. Precambrian Res. Unit, Univ. Cape Town, Bull. 17, 185p.

Kalsbeek, R., & Leake, B.E. (1970) The chemistry and origin of some basement amphibolites between Ivigut and Frederikshäb, southwest Greenland. Gronl. Geol. Undersog. Bull. 80, 5-36.

Kanehira, K., & Tatsumi, T. (1970) Bedded cupriferous iron sulphide deposits in Japan, a review. In : Tatsumi, T. (ed.) Volcanism and ore genesis. Univ. Tokyo Press. Tokyo, 51-76.

Klein, C. (1968) Coexisting amphiboles. J. Petrology, 9, 281-330.

_____ (1969) Two amphibole assemblages in the system actinolite-hornblende-glaucophane. Am. Mineralogist, 54, 212-237.

Kröner, A. (1974) Note on the alleged occurrence of pillow lavas in the southern Damara Belt. Precambrian Res. Unit, Univ. Cape Town, Bull. 15, 177-182.

_____ (ed.) (1974) Proposal for the stratigraphic classification and nomenclature of rocks presently considered to be post-Waterberg/pre-Cape age. Unpubl. Rep., S.A. Comm. Stratigr. working group post-Waterberg/pre-Cape, 10p.

Leake, B.E. (1964) The chemical distinction between ortho- and para-amphibolites. Jour. Petrology, 5, 238-254.

MacDonald, G.A., & Katsura, T. (1964) Chemical composition of Hawaiian lavas. Jour. Petrology, 5, 82-133.

Martin, H. (1965) The precambrian geology of South West Africa and Namaqualand. Precambrian Res. Unit, Univ. Cape Town, 159p.

Mehnert, K.R. (1969) Composition and abundance of common metamorphic rocks. In : Wedepohl, K.H. (ed.), Handbook of Geochemistry. Springer-Verlag, Berlin., 1, 272-296.

Miyashiro, A. (1975) Classification, characteristics, and origin of ophiolites. Jour. Geology, 83, 249-281.

Norman, M.B. (1974) Improved techniques for selective staining of feldspar and other minerals using amaranth. Jour. of Res., U.S. Geol. Surv., 2, 73-79.

Orville, P.M. (1969) A model for metamorphic differentiation origin of thin layered amphibolites. Amer. Jour. Sci., 267, 64-86.

Pearce, J.A., & Cann, J.R. (1973) Tectonic setting of basic volcanic rocks determined using trace element analyses. Ear. Planet. Sci. Lett., 19, 290-300.

Pearce, T.H., Gorman, B.E., & Birkett, T.C. (1975) The TiO_2-K_2O-P_2O_5 diagram : a method of discriminating between oceanic and non-oceanic basalts. Ear. Planet. Sci. Lett., 24, 419-426.

Philpots, J.A., Schnetzler, C.C., & Hart, S.R. (1969) Submarine basalts : some K, Rb, Sr, Ba, rare-earth, H_2O and CO_2 data bearing on their alteration, modification by plagioclase and possible source materials. Ear. Planet. Sci. Lett., 7, 293.

Poldervaart, A. (1955) Chemistry of the earth's crust. Geol. Soc. Am. Spec. Paper, 62, 119-144.

Preto, V.A.G. (1970) Amphibolites from the Grand Forks Quadrangle of British Columbia, Canada. Geol. Soc. Am. Bull., 81, 763-782.

Puhan, D., & Hoffer, E. (1973) Phase relations of talc and tremolite in metamorphic calcite-dolomite sediments in the Southern portion of the Damara belt (S.W.A.). Contrib. Mineral. Petrol., 40, 207-214.

Ramsay, J.G. (1967) Folding and fracturing of rocks. McGraw-Hill Book Co., New York, 568p.

Rimsaite, J. (1974) Mineral assemblages and low-grade metamorphic-metasomatic alterations in an archean greenstone belt, Malartic, Quebec. Can. Mineralogist, 12, 520-526.

Shackleton, R.M. (1969) Displacement within continents. In : Kent, P.E. et al. (eds.), Time and place in orogeny. Geol. Soc. London, London, 1-7.

_____ (1973) Correlation of structures across Precambrian orogenic belts in Africa. In : Tarling, D.H. & Runcorn, S.K. (eds.), Implications of continental drift to the earth sciences, 2. Academic Press, London, 1091-1094.

Shaw, D.M., & Kudo, A.M. (1965) A test of the discriminant function in the amphibolite problem. Mineralog. Mag., 34, 423-435.

Shido, R. (1958) Plutonic and metamorphic rocks of the Nakoro and Iritono districts in the central Abukuma Plateau. Jour. Facult. Sci. Univ. Tokyo, 11, 131-217.

Sillitoe, R.H. (1972) Formation of certain massive sulphide deposits at sites of sea-floor spreading. Trans. Inst. Min. Metall., B, 81, B141-B147.

Tatsumi, T., Sekine, Y., & Kanehira, K. (1970) Mineral deposits of volcanic affinity in Japan : metallogeny. In : Tatsumi, T. (ed.) Volcanism and ore genesis. Univ. Tokyo Press. Tokyo, 3-50.

Turner, F.J., & Verhoogen, J. (1960) Igneous and metamorphic petrology. McGraw-Hill Book Co., New York, 694p.

_____ (1968) Metamorphic petrology. McGraw-Hill Book Co., New York, 403p.

Viljoen, R.P. & Viljoen, M.J. (1969) The effects of metamorphism and serpentinization of the volcanic and associated rocks of the Barberton region. Geol. Soc. S. Afr., Spec. Pub., 2, 29-54.

_____ & _____ (1969) Evidence for the composition of the primitive mantle and its products of partial melting from a study of the rocks of the Barberton Mountain Land. Geol. Soc. S. Afr. Spec. Pub., 2, 275-296.

_____ & _____, Grootenboer, J., Longshaw, T.G. (1975) ERTS-1 imagery : applications in geology and mineral exploration. Miner. Sci. Engng., 7, 132-168.

Wagner, P.A. (1916) The geology and mineral industry of South West Africa. Geol. Surv. of S.A. Memoir No. 7.

Weaver, S.D., Sceal, J.S.C., & Gibson, I.L. (1972) Trace-element data relevant to the origin of trachytic and pantelleritic lavas in the East African Rift System. Contrib. Mineral. Petrol., 36, 181-194.

Winkler, H.G.F. (1974) Petrogenesis of metamorphic rocks. Springer-Verlag, Berlin, 320p.

Wolf, K.H., Easton, A.J., & Warne, S. (1967) Techniques of examining and analysing carbonate skeletons, minerals and rocks. In : Chilingar, G.V., Bissett, H.J. & Fairbridge, R.W. (eds.), Carbonate Rocks, Physical and Chemical aspects. Elsevier, Amsterdam, 253-341.

Yoder, H.S., & Tilley, C.E. (1962) Origin of basaltic magmas : an experimental study of natural and synthetic rock systems. Jour. Petrology, 3, 342-532.